






Article

LXR α Regulates ChREBP α Transactivity in a Target Gene-Specific Manner through an Agonist-Modulated LBD-LID Interaction

Qiong Fan ¹, Rikke Christine Nørgaard ², Ivar Grytten ³, Cecilie Maria Ness ²,
Christin Lucas ², Kristin Vekterud ¹, Helen Soedling ², Jason Matthews ²,
Roza Berhanu Lemma ⁴, Odd Stokke Gabrielsen ⁴, Christian Bindsbøll ¹, Stine Marie Ulven ²,
Hilde Irene Nebb ², Line Mariann Grønning-Wang ² and Thomas Sæther ^{1,*}

¹ Department of Molecular Medicine, Institute of Basic Medical Sciences, Faculty of Medicine, University of Oslo, N-0317 Oslo, Norway; qiong.fan@medisin.uio.no (Q.F.); kristin.vekerud@medisin.uio.no (K.V.); christian.bindesboll@gmail.com (C.B.)

² Department of Nutrition, Institute of Basic Medical Sciences, Faculty of Medicine, University of Oslo, N-0317 Oslo, Norway; rikkechristine@hotmail.com (R.C.N.); ceciliem.ness@gmail.com (C.M.N.); christin.zwafink@gmail.com (C.L.); helensoedling@gmail.com (H.S.); jason.matthews@medisin.uio.no (J.M.); smulven@medisin.uio.no (S.M.U.); h.i.nebb@medisin.uio.no (H.I.N.); lmgronningwang@gmail.com (L.M.G.-W.)

³ Department of Informatics, Faculty of Mathematics and Natural Sciences, University of Oslo, N-0317 Oslo, Norway; ivargry@student.matnat.uio.no

⁴ Department of Biosciences, Faculty of Mathematics and Natural Sciences, University of Oslo, N-0317 Oslo, Norway; r.b.lemma@ncmm.uio.no (R.B.L.); o.s.gabrielsen@ibv.uio.no (O.S.G.)

* Correspondence: thomas.sather@medisin.uio.no; Tel.: +47-22-851510

Received: 26 March 2020; Accepted: 7 May 2020; Published: 13 May 2020



Abstract: The cholesterol-sensing nuclear receptor liver X receptor (LXR) and the glucose-sensing transcription factor carbohydrate responsive element-binding protein (ChREBP) are central players in regulating glucose and lipid metabolism in the liver. More knowledge of their mechanistic interplay is needed to understand their role in pathological conditions like fatty liver disease and insulin resistance. In the current study, LXR and ChREBP co-occupancy was examined by analyzing ChIP-seq datasets from mice livers. LXR and ChREBP interaction was determined by Co-immunoprecipitation (CoIP) and their transactivity was assessed by real-time quantitative polymerase chain reaction (qPCR) of target genes and gene reporter assays. Chromatin binding capacity was determined by ChIP-qPCR assays. Our data show that LXR α and ChREBP α interact physically and show a high co-occupancy at regulatory regions in the mouse genome. LXR α co-activates ChREBP α and regulates ChREBP-specific target genes *in vitro* and *in vivo*. This co-activation is dependent on functional recognition elements for ChREBP but not for LXR, indicating that ChREBP α recruits LXR α to chromatin *in trans*. The two factors interact via their key activation domains; the low glucose inhibitory domain (LID) of ChREBP α and the ligand-binding domain (LBD) of LXR α . While unliganded LXR α co-activates ChREBP α , ligand-bound LXR α surprisingly represses ChREBP α activity on ChREBP-specific target genes. Mechanistically, this is due to a destabilized LXR α :ChREBP α interaction, leading to reduced ChREBP-binding to chromatin and restricted activation of glycolytic and lipogenic target genes. This ligand-driven molecular switch highlights an unappreciated role of LXR α in responding to nutritional cues that was overlooked due to LXR lipogenesis-promoting function.

Keywords: glucose; cholesterol; lipid metabolism; nuclear receptors; liver; trans-coactivation; ChIP

1. Introduction

Glucose and lipid metabolism are tightly connected and coordinately regulated in mammals to maintain whole-body energy homeostasis. In the liver, excess dietary carbohydrates are converted to fatty acids through *de novo* lipogenesis (DNL) destined for long-term storage as triglycerides in adipose tissue. Dysregulation of lipogenesis contributes to non-alcoholic fatty liver disease (NAFLD), which is associated with increased risk of metabolic syndrome and type 2 diabetes [1,2]. Several transcription factors (TFs) play essential roles in modulating glucose and lipid metabolism, including the cholesterol-sensing nuclear receptor liver X receptor (LXR) and the glucose-sensing TF carbohydrate responsive element-binding protein (ChREBP) [3,4].

While showing high sequence homology, the two LXR subtypes differ in their distribution (reviewed in Reference [5]): LXR α is predominantly expressed in metabolically active tissues, for example, liver and adipose tissue, while LXR β is ubiquitously expressed [6]. Both isoforms heterodimerize with retinoid X receptors (RXRs) and regulate expression of genes involved in cholesterol homeostasis, lipid and glucose metabolism and inflammation [5,7–10], by binding to LXR response elements (LXREs; two direct repeats AGGTCA spaced by four nucleotides, DR4 elements) in gene regulatory regions [11]. *in vivo* LXR transactivity is modulated by oxysterols (oxidized cholesterol derivatives), which bind to the ligand-binding domain (LBD) of LXR [12]. This elicits conformational changes in LBD which leads to the release of co-repressors, recruitment of co-activators and initiation of target gene transcription [13–15]. By functioning as a ‘metabolic sensor,’ LXR can integrate metabolic signals into complex transcriptional responses. In the liver, LXR responds to cholesterol, insulin and glucose in the form of O-linked β -*N*-acetylglucosamine (O-GlcNAc) [12,16–18], by activating the transcription of ChREBP and sterol regulatory element-binding protein (SREBP)-1c [19,20], which alone or together with LXR induce the transcription of glycolytic and lipogenic enzymes, such as liver pyruvate kinase (*Lpk*), acetyl-CoA carboxylase (*Acc*), fatty acid synthase (*Fasn*) and stearoyl-CoA desaturase-1 (*Scd1*) [20–22]. This leads to increased *de novo* synthesis of fatty acids. The discovery of the O-GlcNAc modification of LXR [18] and its activating effects resolved a controversial issue sparked by Mitro et al. [23], proposing that glucose, as a hydrophilic molecule, could act as a direct agonistic ligand for LXR. Several synthetic ligands targeting LXR have been developed, such as the nonsteroidal agonists GW3965 and T0901317 [8,24]. However, none of these have so far reached the clinic, as one of the concerns has been LXR-induced lipogenesis [25,26].

ChREBP is a glucose-activated TF that belongs to the basic helix-loop-helix leucine zipper (bHLH/Zip) family [27]. ChREBP and its obligate partner Max-like protein X (MLX) heterodimerize via the bHLH/ZIP domain of ChREBP (illustrated in Figure 4A) [28] and bind to the conserved consensus sequence carbohydrate response element (ChoRE) located in the promoter region of glucose-responsive genes [29]. The ChoRE is comprised of two E-box (CACGTG) or E-box-like sequences spaced by five nucleotides [30]. The dominant isoform ChREBP α contains a glucose-sensing module (GSM) in its N-terminus, comprised of a low glucose inhibitory domain (LID) and a glucose response activation conserved element (GRACE) (illustrated in Figure 4A) [31]. Under low glucose condition, ChREBP α transactivity is restrained by an intramolecular inhibitory mechanism, involving LID and GRACE [32,33]. Once intracellular glucose levels increase, the inhibition is relieved, either through the direct binding of one or more glucose metabolites to LID, and/or the recruitment of co-regulatory proteins activating ChREBP α [33–36]. In contrast, the shorter isoform ChREBP β , which is transactivated by ChREBP α through an alternative promoter 17 kb upstream of the *Chrebp α* transcription start site (TSS), lacks most of LID (the first 177 amino acids), has escaped glucose regulation and acts constitutively independent of glucose concentration [37]. In addition, glucose activates ChREBP via O-GlcNAc modification, leading to increased ChREBP transcriptional activity and recruitment to target gene promoters [38,39].

We previously reported that LXR deficiency leads to reduced ChREBP activity, resulting in reduced hepatic expression of ChREBP-specific target genes *Pklr* (*Lpk*) and *Mlxipl* (*Chrebp β*) and less ChREBP recruitment to the *Lpk* promoter [16]. Moreover, LXR α is essential in regulating ChREBP activity in

the livers of mice fed a high-glucose diet [40]. Recently, it was also shown that LXR regulates the expression of *Lpk* in the livers of mice fed an oleic acid-enriched diet [41]. It is, however, not clear whether LXR regulates ChREBP-specific target genes indirectly by activating *Chrebp α* expression or directly by modulating ChREBP α activity.

In the current study, we demonstrate that LXR α and ChREBP α interact physically and show a high co-occupancy at regulatory regions in the mouse genome. Moreover, LXR α regulates ChREBP α transactivity in a target gene-specific manner through an agonist-modulated LBD-LID interaction, where LXR α ligand binding restricts the activation of glycolytic and lipogenic target genes. We speculate that this novel function of LXR α as a ligand-driven molecular switch for ChREBP, has been overlooked due to LXR's role in promoting DNL.

2. Materials and Methods

2.1. Materials

Formaldehyde (F1635), the synthetic LXR agonist GW3965 (G6295), dimethyl sulfoxide (DMSO; D4540), Dulbecco's Modified Eagle's Medium (DMEM; D6546), fetal bovine serum (FBS) (F7524), L-glutamine (G7513), penicillin-streptomycin (P4458), insulin (I9278) and D-(+)-glucose solution (G8769) were purchased from Sigma-Aldrich (St. Louis, MO, USA). Tularik (T0901317) was from Enzo Life Sciences (Farmingdale, NY, USA). DMEM, no glucose (11966-025) was purchased from Gibco, Thermo Fisher Scientific (Waltham, MA, USA). Dual Luciferase@reporter assay system (E1960) was purchased from Promega (Madison, WI, USA). All other chemicals were of the highest quality available from commercial vendors.

2.2. ChIP-seq Data Analysis

To generate a genome-wide map of ChREBP and LXR binding sites, two published ChIP-seq datasets were reanalyzed—ChREBP ChIP-seq data from mouse liver (C57Bl/6J male mice were fasted and high-carbohydrate refed to maximize ChREBP chromatin occupancy) [42] and LXR ChIP-seq data from mouse liver (NCBI GSE35262; C57Bl/6 female mice were treated with LXR agonist (T0901317, 30 mpk, 14 days) and anti-pan-LXR polyclonal antibody was used to capture LXR α/β) [43].

Reads were mapped to the mm9 reference genome (Assembly number: MGSCv37) using *BWA aln* (v.0.7.17) with default parameters and alignments with mapping quality less than 30 were discarded using *Samtools filter* (v.1.9). Peaks were called using *MACS* (v.2.1.1) with default parameters. Peaks within mm9 blacklisted regions [44] were discarded. There were 48 647 ChREBP peaks detected and the top 20 000 peaks with highest score were chosen for further analysis. There were 24 728 LXR peaks detected, all of which were chosen for further analysis.

Pairs of close ChREBP and LXR peaks were selected by running *bedtools closest* (v.2.26.0) on the peak summits of the ChREBP and LXR peaks and discarding pairs of close peaks with summit-to-summit distance larger than 1000 base pairs. These pairs were linked to their nearest gene by running *Rgmatch* [45] with *-report gene -distance 25 -promoter 5000* as parameters.

Genomic co-occurrence of the predicted binding sites of the different transcription factors (Figure 1G) was measured by the Forbes coefficient (<https://www.ideals.illinois.edu/handle/2142/55240>) using the Genomic HyperBrowser [46].

2.3. Animals and Fasting-Refeeding Experiments

LXR $\alpha\beta$ wild type, LXR $\alpha^{-/-}$, LXR $\beta^{-/-}$ and LXR $\alpha^{-/-}\beta^{-/-}$ (double knockout, DOKO) male mice were housed in a temperature-controlled (22 °C) facility with a strict 12 h light/dark cycle. The mice had free access to water before and during experiments and normal chow before the experiment. The diet contained 18.5% protein, 4% fat and 55.7% carbohydrate (R36 diet, Lactamin AB, Stockholm, Sweden). LXR α and β -deficient mice and corresponding controls had mixed genetic backgrounds based on 129/Sv and C57BL/6J strains and were backcrossed in C57BL/6J mice (B & K Universal Ltd, Sollentuna,

Sweden) for six generations. The generation of the $LXR\alpha^{-/-}$, $LXR\beta^{-/-}$ and the DOKO mice have been described previously [47,48].

Male mice aged 8–12 weeks (weight 25–30 g) were fasted for 24 h (Fasted) or fasted for 24 h and refed for 12 h (Refed). All male littermates in a litter of correct age, weight and genotype were randomly allocated to a given treatment. No particular measures were taken to minimize subjective bias during group allocation. Each genotype-treatment group consisted of 5–8 animals, 53 mice in total, allowing us to detect 2-fold changes, given a coefficient of variation of 25% or less [49]. The mice were euthanized by cervical dislocation at the end of the dark period. Livers were dissected and rapidly frozen in liquid nitrogen and stored at -80°C until isolation of total RNA. The liver samples were coded and processed by two independent, blinded researchers during RNA sample preparation and quantitative real-time polymerase chain reaction (qRT-PCR). All animal use was approved and registered by the Norwegian Animal Research authority and the regional ethical committee for animal experiments in Sweden.

2.4. Mouse Primary Hepatocytes Isolation and Culture

Mouse primary hepatocytes were isolated as previously described with modest changes [50]. Briefly, male C57BL/6N mice (Jackson Laboratory, Bar Harbor, ME, USA) aged 7–8 weeks were anaesthetized with isoflurane (AbbVie, North Chicago, IL, USA), before the livers were perfused via the portal vein with liver perfusion medium (#17701038, Thermo Fisher Scientific, Bleiswijk, The Netherlands) for 15 min (2 mL/min) followed by liver digestion medium (#17703034, Thermo Fisher Scientific, Bleiswijk, The Netherlands) for 15 min. The liver was then removed and dissociated in liver perfusion buffer before filtering through a 100 μM strainer (Thermo Fisher Scientific, Bleiswijk, The Netherlands). Hepatocytes were washed 4 times with ice-cold low glucose DMEM (D6046; Sigma-Aldrich, St. Louis, MO, USA) supplemented with 10 mM Hepes (#15630080, Thermo Fisher Scientific, Bleiswijk, The Netherlands), 5% charcoal stripped FBS (#12329782, Thermo Fisher Scientific, Bleiswijk, The Netherlands) and 1% penicillin-streptomycin (50 U/mL; 50 $\mu\text{g}/\text{mL}$). Hepatocytes were seeded at 2.5×10^5 cells/well onto type I collagen coated 12-well plates in attachment medium (William's E media, #12551032, Thermo Fisher Scientific, Bleiswijk, The Netherlands) with 10% FBS, 1% penicillin-streptomycin and 10 nM insulin. The medium was changed 2 h after plating to overnight media consisting of low glucose DMEM (D6046; Sigma-Aldrich, St. Louis, MO, USA), 5% FBS, 1% penicillin-streptomycin and 1 nM insulin. On the next day, hepatocytes were washed twice with 1 mL medium/well consisting of DMEM with either 1 mM glucose (LG) or 25 mM glucose (HG), 5% FBS, 1% penicillin-streptomycin and 1 nM insulin and then cultured overnight in LG or HG medium supplemented with 0.1% DMSO, 10 μM GW3965 or 10 μM T0901317, respectively. Hepatocytes were harvested after 18 h treatment for RNA isolation.

2.5. Cell Culture and Transfection

Huh7 human liver hepatoma cells [51] and COS-1 fibroblast-like cells derived from African green monkey kidney (ATCC, CRL-1650TM) were maintained in 25 mM glucose DMEM (D6546; Sigma-Aldrich, St. Louis, MO, USA) supplemented with 10% fetal bovine serum, 4 mM L-Gln and 1% penicillin/streptomycin. AML12 mouse liver non-cancerous cells (ATCC, CRL-2254TM) were maintained in DMEM/F12 (#31331, Gibco, Thermo Fisher Scientific, Bleiswijk, The Netherlands) supplemented with 10% fetal bovine serum, 1% penicillin/streptomycin, 0.1% insulin, transferrin, and sodium selenite (ITS) (I3146; Sigma-Aldrich, St. Louis, MO, USA) and 0.1 μM dexamethasone (D2915; Sigma-Aldrich, St. Louis, MO, USA). All cells were maintained at 37°C in humidified atmosphere of 5% CO_2 in air and routinely tested for mycoplasma contamination. Cells were transfected with indicated plasmids using Lipofectamine 2000 (#10696153, Thermo Fisher Scientific, Bleiswijk, The Netherlands).

2.6. Plasmids

The FLAG-tagged human or mouse LXR expressing plasmids pcDNA3-FLAG-hLXR α , pcDNA3-FLAG-hLXR β and pcDNA3-FLAG-mLXR α , the untagged human RXR α expressing plasmid pcDNA3-hRXR α and the empty vector pcDNA3-FLAG have been described earlier [18,52]. To generate the pcDNA3-FLAG-hLXR α -DBD-mutant, two cysteine to alanine point mutations (C115A/C118A) in the DNA binding domain were introduced using the QuikChange Site-directed Mutagenesis kit (Agilent Genomics, Santa Clara, CA, USA) and the primers listed in Supplemental Table S1. The plasmids expressing mouse Mlx γ (pCMV4-HA-mMlx γ), ChREBP α (pCMV4-FLAG-mChREBP α) and ChREBP β (pCMV4-FLAG-mChREBP β), as well as the empty vector pCMV4, were received as generous gifts from Prof. Mark Herman [37]. To generate the ChREBP α LID expression plasmid, cDNA corresponding to the FLAG-tag, ChREBP α amino acids 1–178 and a stop codon, was PCR amplified from pCMV4-FLAG-mChREBP α using specific primers (Supplemental Table S1), and subcloned into the pCMV4 vector using BglIII and HindIII restriction enzymes. The plasmid expressing the ChREBP quadruple mutant (H51A/S56D/ F90A/N278A) (ChREBP-Q) was a kind gift from Prof. Em. Howard Towle [32]. Accession numbers of the DNA sequences are listed as below: human LXR α , NM_005693.4; human LXR β , NM_007121.7; mouse LXR α , NM_013839.4; human RXR α , NM_002957.6; mouse ChREBP α , NM_021455.5; mouse Mlx γ , NM_011550.3.

The *Chrebp* β promoter-driven luciferase reporter pGL3b-ChREBP β -exon1b-luc (wild-type) and its mutants ChoRE+Ebox-del (both ChoRE and E-box deleted) and ChoRE-del (ChoRE deleted) were kind gifts from Prof. Mark Herman [37]. The pGL3b-ChREBP β -exon1b-luc reporter mutants Ebox-del (E-box deleted) and DR4-del (candidate DR4 response element deleted) were generated using the QuikChange Site-directed Mutagenesis kit (Agilent Genomics, Santa Clara, CA, USA) and the primers listed in Supplemental Table S1. The pGL3-rL-PK(-183)-luc (PK-luc) was a kind gift from Prof. Em. Howard Towle [53] and the ChoRE mutated reporter pGL3-rL-PK(-183)-Gal4-luc (PK-ChoREmut-luc) was a kind gift from Prof. Donald K. Scott [54]. The mouse SREBP1c reporter pGL2basic/-550-mSREBP1c-prom-luc (SREBP1c-luc) was kindly provided by Prof. Nobuhiro Yamada [55].

The multimerized ChoRE and LXRE reporters: pGL3b-2xChoRE-2xLXRE-10 (ChoRE+LXRE-luc), pGL3b-2xChoRE-10 (ChoRE-only-luc) and pGL3b-2xLXRE-10 (LXRE-only-luc) were constructed in two steps—first, the 136 bp inserts were made by gene synthesis (GenScript, Nanjing, China). The SacI-BglIII-lined inserts were designed to contain two canonical ChoREs (CACGTGatataCACGTG) and two canonical LXREs (AGGTCActctAGGTC) in the order ChoRE-LXRE-ChoRE-LXRE and with a spacing of 10 bp (gtaataataa), giving a phasing of ~20 bp center to center between the REs. The inserts were then cut from the production vector pUC57 (GenScript, Nanjing, China) and subcloned into pGL3 basic vector between SacI and BglIII. The schematic representation of synthetic reporters is illustrated in Figure 3A. The Renilla Luciferase reporter pRL-CMV (Promega, Madison, WI, USA) was used as internal control of transfection efficiency. All plasmids were verified by sequencing.

2.7. Luciferase Reporter Assay

Huh7 cells were seeded at density 7×10^4 cells/well in 24-well plates. After 24 h, cells were transfected with 300 ng of luciferase reporters, 150 ng of LXR/RXR and/or 150 ng of ChREBP/Mlx expressing plasmids or empty controls pcDNA3-FLAG and pCMV4. Renilla luciferase reporter (pRL-CMV; 50 ng) was included as an internal control for transfection efficiency. All transfections were performed with Lipofectamine 2000. Dual luciferase reporter assay was performed 24 h post transfection as previously described [16]. Transfections were verified by immunoblotting. For LXR agonist treatment, synthetic ligand GW3965 (1 μ M or 10 μ M) or T0901317 (5 μ M) was applied to cells 6 h post transfection and 0.1% DMSO was used as control. For low vs high glucose (2.5 mM vs 25 mM) treatment, cells were transfected in high glucose and 6 h post transfection cells were washed twice with low or high glucose medium, respectively and then cultured in corresponding medium for 18 h. After 18 h of incubation, cells were washed with PBS and lysed in Passive Lysis Buffer (Promega, Madison, WI, USA). Dual-Luciferase® Reporter Assays (Promega, #E1960) were run on a Synergy

H1 plate reader (BioTek® Instruments, Winooski, VT, USA) according to the manufacturer's manual. Readings of Firefly Luciferase were normalized to the Renilla Luciferase readings and data from at least three independent transfections experiments run in quadruplicates are presented.

2.8. Chromatin Immunoprecipitation (ChIP)

Huh7 cells were transfected with the ChoRE+LXRE reporter and plasmids expressing ChREBP α , ChREBP-Q or ChREBP β and Mlx γ . AML12 cells were transfected with plasmids expressing ChREBP α , Mlx γ , with or without LXR α and RXR α . For LXR agonist treatment, 10 μ M of GW3965 was applied to cells 6 h post transfection and 0.1% DMSO was used as control. Twenty-four hours post transfection, cells were cross-linked with 1% formaldehyde for 10 min at room temperature, followed by 5 min incubation with 125 mM glycine to quench the reaction. Cells were washed twice in cold PBS and harvested in PBS-T. The cell pellets were lysed in lysis buffer (0.1% SDS, 1% Triton X-100, 0.15 M NaCl, 1 mM Ethylenediaminetetraacetic acid (EDTA) and 20 mM Tris (pH 8.0)). The lysed cells were sonicated to get an average size of 200–500 bp chromatin fragments using a Bioruptor (Diagenode, Seraing, Belgium). Chromatin was immunoprecipitated with 4 μ g antibody against ChREBP (NB400-135; Novus Biologicals Centennial, CO, USA), against LXR (antibody generation described in Reference [56]), or rabbit IgG (011-000-002; Jackson ImmunoResearch Laboratories, West Grove, PA, USA) over night at 4 °C. Protein A Dynabeads were washed four times in lysis buffer, added to the chromatin and rotated at 4 °C for 2 h. The Dynabeads were then washed three times with wash buffer 1 (0.1% SDS, 1% Triton X-100, 0.15 M NaCl, 1 mM EDTA, 20 mM Tris (pH 8)), followed by washing once in wash buffer 2 (0.1% SDS, 1% Triton X-100, 0.5 M NaCl, 1 mM EDTA, 20 mM Tris (pH 8)), once in wash buffer 3 (0.25 M LiCl, 1% NaDOC, 1% NP-40, 1 mM EDTA, 20 mM Tris (pH 8)) and finally once in wash buffer 1. All washing steps were done with rotation for 5 min at room temperature. DNA-protein complexes were eluted with 1% SDS and reverse cross-linked over night at 65 °C. DNA was purified by using the QIAquick PCR Purification Kit (#28104; QIAGEN, Hilden, Germany). DNA enrichment was quantified by qRT-PCR. ChIP primer sequences are listed in Supplementary Table S3.

2.9. RNA Extraction, cDNA Synthesis and Quantitative RT-PCR

RNA was isolated with TRIzol® reagent (#15596018, Invitrogen, Thermo Fisher Scientific, Waltham, MA, USA) according to the manufacturer's protocol, including a high salt (0.8 M sodium acetate, 1.2 M NaCl) precipitation step to avoid contaminating polysaccharides to co-precipitate with RNA. Extracted RNA was further purified using RNeasy spin columns (#74104, QIAGEN, Hilden, Germany). Isolated RNA (500 ng) was reverse transcribed into cDNA using MultiScribe Reverse Transcriptase (#4311235, Thermo Fisher Scientific, Bleiswijk, The Netherlands) and random hexamer primers. RT-qPCR was performed with 1 μ L of the cDNA synthesis reaction using Kapa SYBR FAST qPCR Master Mix (KapaBiosystems, Roche, Basel, Switzerland) on a Bio-Rad CFX96 Touch™ Real-Time PCR Detection System (Bio-Rad Laboratories, Hercules, CA, USA). Assay primers were designed with Primer-BLAST software (NCBI, Bethesda, MD, USA) [57]. Gene expression was calculated using the $2^{-\Delta\Delta CT}$ method and normalized against the expression of TATA-binding protein (*Tbp*). All primer pairs showed an efficiency of 90–110% at $R^2 > 0.98$. Primer sequences are listed in Supplementary Table S2.

2.10. Co-Immunoprecipitation (CoIP)

COS-1 cells were transfected with plasmids expressing ChREBP α full-length (FL) or N-terminal LID truncation or ChREBP β , with or without LXR α FL or truncations (amino acids: 1–166, 95–447 and 166–447) or LXR β . For ChREBP β transfections we used 6-fold more DNA than of ChREBP α to obtain comparable protein levels in the CoIP. For LXR agonist treatment, 0.1% DMSO or GW3965 (1 μ M) was applied to cells 6 h post transfection. Cells were harvested 24 h post transfection and lysed in lysis buffer (200 mM NaCl, 20 mM HEPES (pH 7.4), 1% NP-40) containing 1 mM NaF, 1 mM Na₃VO₄, 1 mM β -glycerophosphate and Complete™ protease inhibitors (Roche Applied Science, Penzberg, Germany), followed by snap freezing on dry ice to disrupt nuclear membranes. The lysates

were then thawed on ice, cleared by centrifugation at $17,000\times g$, 10 min and immunoprecipitated with 2 μg ChREBP (NB400-135, Novus Biologicals, Littleton, CO, USA), LXR α (PP-PPZ0412; R&D Systems, Minneapolis, MN, USA) or LXR β (PP-K8917; R&D Systems, Minneapolis, MN, USA) antibodies bound to protein A Dynabeads (Invitrogen, Thermo Fisher Scientific, Waltham, MA, USA) for 2 h at 4 °C. Beads were washed three times in wash buffer (200 mM NaCl, 20 mM HEPES (pH 7.4), 0.1% NP-40) with 5 min rotation in between, before proteins were eluted from the beads with $1\times$ SDS loading buffer at 95 °C for 5 min. Co-immunoprecipitated proteins were analyzed by immunoblotting.

2.11. Immunoblotting

Proteins were separated by Sodium dodecyl sulfate polyacrylamide gel electrophoresis (SDS-PAGE) (Bio-Rad, Hercules, CA, USA) and blotted onto PVDF membrane (MerckMillipore, Darmstadt, Germany). Primary antibodies used were LXR α (PP-K8607, R&D systems; 1:1000), LXR α LBD (PP-PPZ0412-00, R&D systems, Minneapolis, MN, USA; 1:1000), LXR β (PP-K8917-00, R&D systems, Minneapolis, MN, USA; 1:1000), RXR α (sc-553, Santa Cruz Biotechnology, Dallas, TX, USA; 1:1000), ChREBP (NB400-135, Novus Biologicals, Littleton, CO, USA; 1:1000), FLAG (F1804; Sigma-Aldrich, St. Louis, MO, USA; 1:1000) and β -actin (A5441; Sigma-Aldrich, St. Louis, MO, USA; 1:1000). Secondary antibodies used were horseradish peroxidase-conjugated goat anti-mouse IgG or mouse anti-rabbit IgG (115-035-174 and 211-032-171, Jackson ImmunoResearch Laboratories, West Grove, PA, USA; both 1:10,000).

2.12. Statistical Analysis

Statistical analyses were performed using GraphPad Prims 8 (GraphPad Software Inc., San Diego, CA, USA). All data were presented as means and standard error of the mean (SEM). In addition, all individual data points are plotted. Data distribution and similarity in variance between groups were analyzed by Shapiro-Wilk and Brown-Forsythe tests, respectively. Statistical differences between groups were determined by two-way analysis of variance (ANOVA) followed by Tukey's multiple comparison tests for data with two variables. For data with one variable we used one-way ANOVA with Dunnett correction to compare every mean to the control mean, alternatively Tukey correction for multiple comparisons. For all statistical tests, $p < 0.05$ was considered statistically significant.

2.13. Gene Set Enrichment Analysis

Gene set enrichment analysis of genes with ChREBP-LXR peak pairs with a peak-to-peak-distance <100 bp, residing in promoters, TSS and first exons (based on the *Rgmatch*; corresponding to -5000 to $+2500$ bp from TSS) were made with the ConsensusPathDB tool from the Max-Planck-Institute for Molecular Genetics (<http://cpdb.molgen.mpg.de/>) [58], using the Reactome Pathway Database (<https://reactome.org>). Minimum overlap with input list was set to 3 and the p -value cutoff to $p < 0.01$.

2.14. Data Availability

The ChIP-seq datasets used in this study is available at NCBI GEO (<https://ncbi.nlm.nih.gov/geo>) under accession number GSM864670 (LXR), GSM1899651 (FXR) and GSM864671 (PPAR α) without any restrictions. The ChREBP ChIP-seq dataset [42] was kindly provided by Prof. Lawrence Chan. Scripts used to perform peak calling and analyze the called peaks are available at <https://github.com/ivargr/open-the-lid-chip-seq-analysis>. The Forbes co-occurrence analysis is available at <https://hyperbrowser.uio.no/hb/u/ivar/h/open-the-lid-co-occurrence-analysis>.

3. Results

3.1. ChREBP α and LXR α Interact and Show a High Co-Occupancy of the Mouse Liver Genome

LXR is one of the factors that regulate ChREBP-dependent transcription in liver. We previously demonstrated that when knocking out LXR in mice, ChREBP loses its ability to bind to carbohydrate

responsive elements (ChoREs), which affects hepatic gene expression of ChREBP-specific targets like *Lpk* and *Chrebpβ* [16]. This can be explained by direct and indirect mechanisms. To better understand how LXR affects ChREBP activity, we asked whether the two TFs could interact. We co-immunoprecipitated (CoIP'ed) LXR and ChREBP in COS-1 cells cultivated in high glucose media (25 mM), to induce the activity of ChREBP α [16,37]. LXR α was detected in the ChREBP immunoprecipitate and reciprocally, ChREBP α was detected when immunoprecipitating with an LXR α antibody (Figure 1A). We next assessed whether this interaction could be detected at the genomic level. To determine this, we reanalyzed two published chromatin immunoprecipitation sequencing (ChIP-seq) datasets; one ChREBP ChIP-seq performed in livers from mice fasted and refed a high-carbohydrate diet [42] and one LXR ChIP-seq done in livers from mice treated with the LXR agonist T0901317 [43]. The sequence reads were mapped to the mouse genome generating a genome-wide, high-resolution map of ChREBP and LXR binding sites. We detected 48,647 and 24,728 binding sites for ChREBP and LXR, respectively.

Using the top 20,000 ChREBP peaks and all the LXR peaks we calculated the peak(ChREBP)-to-peak(LXR) distance for all peaks. Interestingly, as many as 11,022 peak pairs showed a peak-to-peak distance of less than 1000 bp and 7928 (71.9%) of these were less than 100 bp apart (Figure 1B). Given the resolution of these datasets, all peaks less than 100 bp apart are likely to represent co-localized peaks, indicating that ChREBP and LXR occupy many of the same loci and that co-occupancy within these regions is high (Figure 1D). We also found that the peak pairs clustered around transcription start sites (TSSs), with the expected depletion at TSS (Figure 1C). The peak pairs which represent peaks less than 100 bp apart were located both upstream and downstream of TSS. However, we found that peak pairs of *bona fide* LXR or ChREBP target genes (blue dots) located mainly upstream or near the TSS, consistent with the notion that most TF binding sites are found upstream of TSSs [59,60]. As an example, the two ChREBP target genes *Lpk* and *Chrebpβ* showed significant ChREBP enrichment at the expected sites in the respective promoters and LXR co-occupied the same sites (Figure 1E). Looking at the genomic position of all peak pairs, independent of distance to TSS using *Rgmatch* (<https://bitbucket.org/pfurio/rgmatch>), we found the peak pairs to be distributed throughout the genome like other NRs [43,61,62]. Specifically, 39% of them seem to cluster around TSSs (Figure 1F; Promoter-TSS-First Exon-First Intron).

To assess how the seemingly high genome-wide co-occupancy of ChREBP and LXR compared with the co-occupancy between other hepatic TFs, we reanalyzed ChIP-seq data of mouse peroxisome proliferator-activated receptor- α (PPAR α) and farnesoid X receptor (FXR) [43,63]. We next calculated the Forbes coefficients (FC), evaluating genomic co-occurrence while correcting for genome coverage [64]. Both PPAR α and FXR are known to co-occupy genomic loci and/or interact with LXR and ChREBP [43,65–67]. PPAR α and LXR showed the highest similar score among all compared TFs (FC: 136.7; Figure 1G), in line with published data [43]. ChREBP and LXR shared the second highest genomic co-occurrence, with a FC of 133.7 (Figure 1G). FXR was recently reported to physically interact with ChREBP, negatively regulating ChREBP activity [65]. Thus, it was somewhat unexpected to see that FXR shared a significantly smaller portion of the genome with ChREBP than LXR did (FC: 57.5; Figure 1G).

Finally, we performed gene set enrichment analysis (GSEA) based on the Reactome Pathway Database. We analyzed genes with ChREBP-LXR peak pairs residing either in the promoter, around the TSS or in the first exon and with a peak-to-peak-distance <100 bp (corresponding to peak pairs between –5000 to +2500 bp from the TSS). As expected, the filtered genes were enriched in pathways regulated by both ChREBP and LXR, for example, metabolism of lipids, fatty acids and glucose (Table 1). Notably, pathways involved in metabolism of amino acids, γ -carboxylation and coagulation, which has not been described to be regulated by ChREBP nor LXR, were also enriched in the gene set. This suggests potential novel biological functions regulated through the concomitant binding of ChREBP and LXR.

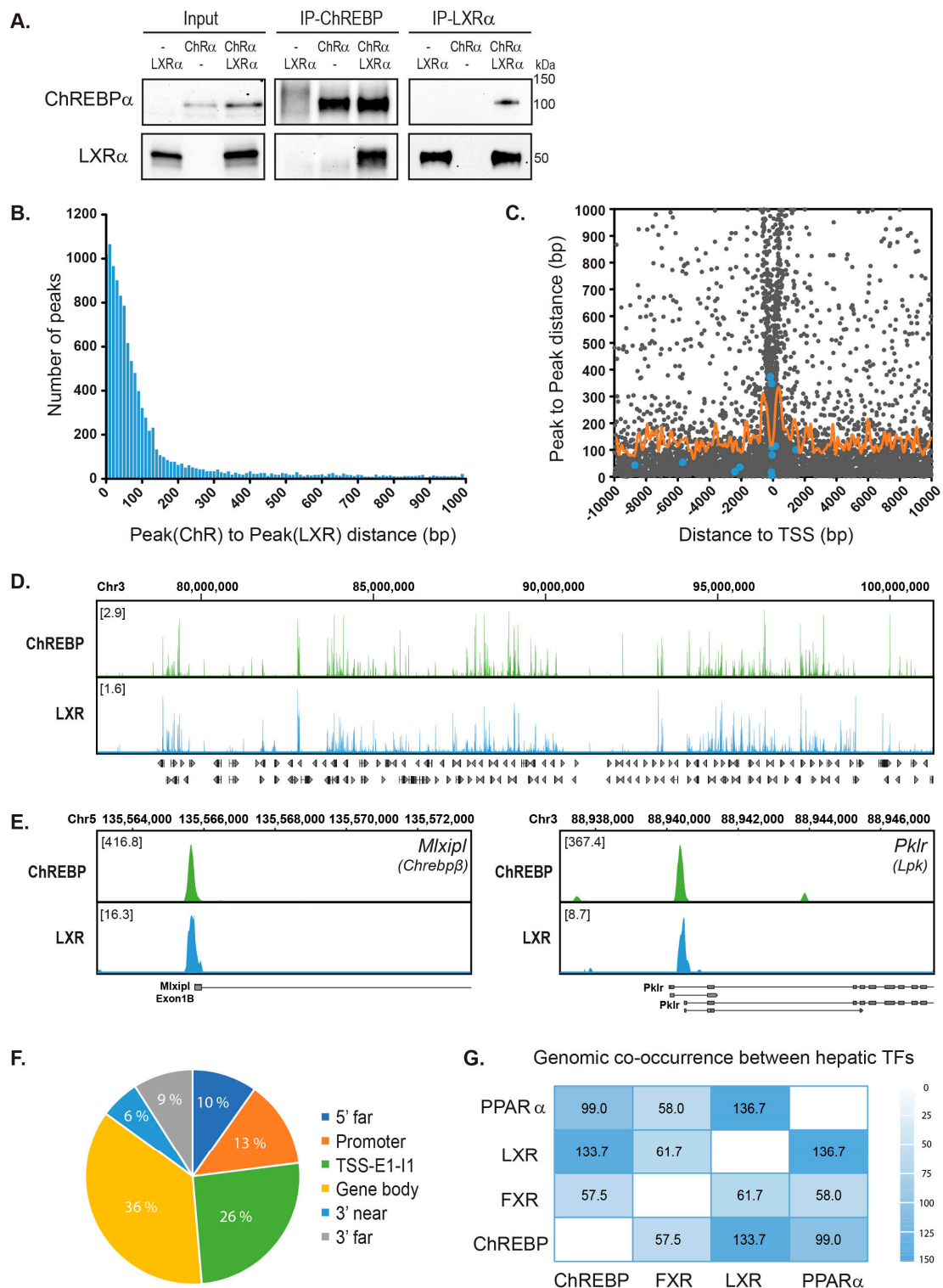


Figure 1. Genome-wide co-occupancy of carbohydrate responsive element-binding protein (ChREBP) and liver X receptor (LXR) in mouse liver. **(A).** Co-immunoprecipitation (CoIP) of LXR α and ChREBP α transfected in COS-1 cells cultured in 25 mM glucose. Lysates were immunoprecipitated with ChREBP and LXR α antibodies and input and immunoprecipitated proteins immunoblotted with the same antibodies ($n = 3$). One representative western blot is shown. **(B).** Distribution of ChREBP-LXR peak pairs. ChREBP ChIP-seq data from fasted and high-carbohydrate refeed mouse liver [42] and LXR ChIP-seq data from T0901317-treated mouse liver [43] were reanalyzed to generate a genome-wide map of ChREBP and LXR binding sites. The top 20,000 peaks from each dataset were used to calculate

the Peak(ChREBP)-to-Peak(LXR) distance and all peak pairs with a peak-to-peak distance <1000 bp were plotted against the number of peak pairs. (C). Localization of ChREBP-LXR peak pairs. The Peak(ChREBP)-to-Peak(LXR) distance were plotted against the distance from mid peak-to-peak position to transcription start site (TSS) of the nearest gene (Distance to TSS). Blue dots, verified LXR/ChREBP target genes, *Acaca*, *MlxiplA*, *MlxiplB*, *Pklr*, *Scd1*, *Srebf1* and *Txnip*. Orange curve, moving average (window: 100 bp) of peak-to-peak distance as a function of distance to TSS. (D). Global landscape of LXR-ChREBP co-occupancy. Browser view of LXR and ChREBP tracks on Chromosome 3. Square brackets indicate the scale maxima of $\log_2(\text{ChIP}/\text{input})$ ratios. (E). Local pattern of LXR-ChREBP co-occupancy. Browser view of LXR and ChREBP tracks on the promoter regions of the ChREBP target genes *Mlxipl* (*ChREBPβ*) and *Pklr* (*Lpk*). Square brackets indicate the scale maxima of ChIP/input ratios. (F). Genomic positions of the ChREBP-LXR peak pairs. The peak pairs were mapped to genomic elements using *Rgmatch*. The elements shown are grouped as follows: 5' far, 25 kb to 5 kb upstream of TSS; Promoter, <5 kb upstream of TSS; TSS, -200 bp to +200 bp; E1, first exon; I1, first intron; Gene body, the whole area of any exon or intron, other than the first exon and the first intron of the gene; 3' near, <5 kb downstream of TSS; 3' far, 5 kb to 25 kb downstream of TSS. (G). Genome-wide co-occurrence of mouse hepatic transcription factors (TFs). Comparison of LXR and ChREBP with published binding profiles of peroxisome proliferator-activated receptor-α (PPARα) [43] and farnesoid X receptor (FXR) [63]. Genomic co-occurrence (to which degree binding sites occur at the same positions in the genome) between ChREBP, LXR, FXR and PPARα were measured by the Forbes coefficients (FC) using the Genomic HyperBrowser.

Table 1. Top 10 pathways enriched in genes with ChREBP-LXR peak pairs.

| Pathway Name | Reactome ID | Candidates | p-Value | LXR | ChREBP |
|----------------------------------------------------------------|-------------|-------------|-----------------------|-----|--------|
| Metabolism | 1430728 | 302 (15.4%) | 3.6×10^{-27} | × | × |
| Metabolism of lipids | 556833 | 113 (17.1%) | 4.6×10^{-13} | × | × |
| Metabolism of amino acids and Derivatives | 71291 | 61 (18.0%) | 2.2×10^{-8} | | |
| Glucose metabolism | 70326 | 24 (26.7%) | 3.9×10^{-7} | × | × |
| γ-carboxylation, transport and N-terminal cleavage of proteins | 159854 | 8 (72.7%) | 3.9×10^{-7} | | |
| Formation of Fibrin Clot | 140877 | 14 (35.9%) | 2.2×10^{-6} | | |
| Fatty acid metabolism | 8978868 | 36 (19.5%) | 2.7×10^{-6} | × | × |
| γ-carboxylation of protein precursors | 159740 | 7 (70.0%) | 3.3×10^{-6} | | |
| Removal of N-terminal propeptides from γ-carboxylated proteins | 159782 | 7 (70.0%) | 3.3×10^{-6} | | |
| Gluconeogenesis | 70263 | 12 (35.3%) | 1.5×10^{-5} | × | × |

Gene filter: promoter to first exon (−5000 to +2500 bp), peak-to-peak distance <100 bp. Symbol × indicates pathways reported to be regulated by LXR and ChREBP in the literature.

3.2. LXRα and ChREBPα Co-Activates ChREBP Target Genes In Vitro and In Vivo

Having established that ChREBPα and LXRα interact and that they co-occupy regulatory regions in the mouse liver genome, we addressed the transcriptional effects of this interaction in reporter gene assays using two luciferase reporter constructs driven by the mouse *ChREBPβ* promoter [37] and the rat *Lpk* promoter [53]. LXR was always co-transfected with its dimerization partner RXRα and ChREBP with its dimerization partner Mlxγ, unless otherwise stated. As expected, ChREBPα:Mlxγ were able to induce the transcription from both reporters in the human hepatocarcinoma cell line Huh7 (Figure 2A). Moreover, ChREBPα transactivation of the *ChREBPβ* promoter increased three-fold when the glucose concentration in the media was augmented from 2.5 mM to 25 mM (Figure 2A). This is consistent with data from the seminal ChREBPβ study by Herman and coworkers [37]. Interestingly, LXRα:RXRα seemed to be able to upregulate the transcriptional activity from both promoters and ChREBPα and LXRα together showed a synergistic effect on the transcriptional activity (Figure 2A). To exclude the potential impact of RXRα in regulating these constructs, we examined RXR and LXR separately and

observed no induction of *Chrebpβ* promoter activity from either RXRα or LXRα alone (Supplementary Figure S1A). In the following in vitro experiments, we chose to keep the glucose concentration at 25 mM to ensure a high ChREBPα activity, unless otherwise stated.

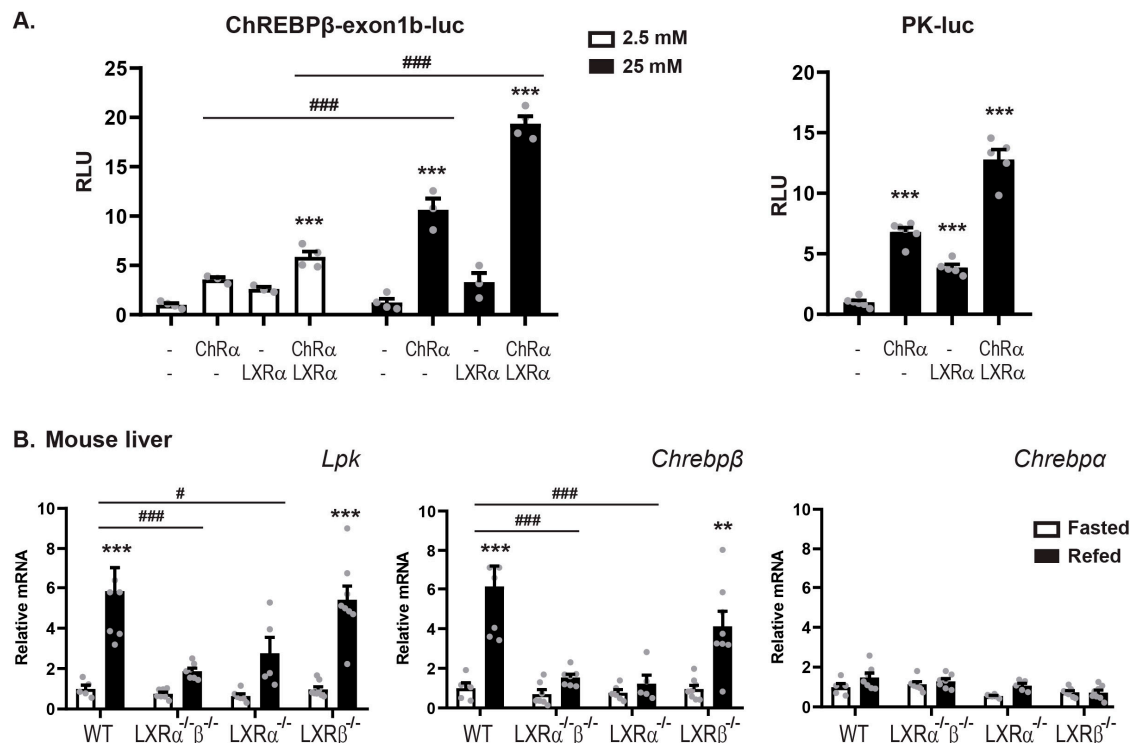


Figure 2. LXRα co-activates ChREBP specific target genes in vitro and in vivo. (A) Huh7 cells cultured in 25 mM glucose were transfected with a *Chrebpβ* ($n = 3$) or *Lpk*-driven luciferase reporter ($n = 6$) and plasmids expressing ChREBPα/Mlxγ, with or without LXRα/RXRα. The Renilla luciferase reporter pRL-CMV was used as internal control. Six hours post transfection, cells were treated with 2.5 mM or 25 mM glucose for 18 h. Dual luciferase reporter assays were performed 24 h post transfection. (B) LXRαβ wild type (WT), LXRα^{-/-}, LXRβ^{-/-} and LXRα^{-/-}β^{-/-} mice were fasted for 24 h (white bars) or fasted for 24 h and refed for 12 h (black bars) ($n = 5–8$ mice per group). Hepatic gene expression of *Lpk* (*Pklr*), *Chrebpβ* and *Chrebpα* was analyzed by quantitative RT-PCR, normalized to *Tbp* and the control group set to 1. For the WT fasted group, Ct values were ≈ 28 for *Chrebpα* and 29 for *Chrebpβ*. Data are presented as mean \pm standard error of the mean (SEM). Significant differences are shown as ** $p < 0.01$, *** $p < 0.001$ compared to control within the same treatment and # $p < 0.05$, ### $p < 0.001$ between indicated groups.

To investigate the impact of the different LXR subtypes, LXRα and LXRβ, on ChREBP activity in vivo, we performed fasting-refeeding experiments with wild-type (WT), LXRα^{-/-}, LXRβ^{-/-} and LXRα^{-/-}β^{-/-} (double knockout, DOKO) mice. The mice were fasted for 24 h or fasted for 24 h and refed for 12 h before they were sacrificed. Liver from 5–8 animal per genotype were examined. The feeding-induced hepatic expression of the ChREBP specific target genes *Lpk* and *Chrebpβ* was significantly reduced in LXRα^{-/-} and DOKO mice but not in LXRβ^{-/-} mice (Figure 2B). On the contrary, no significant changes in *Chrebpα* expression was observed that could explain the different responses to LXRα versus -β knockout seen for the ChREBP target genes, suggesting that LXRα but not LXRβ, is essential to regulate ChREBP activity but not *Chrebpα* expression. This conclusion was substantiated in reporter gene assays, showing no activation of the *Chrebpβ* promoter by LXRβ and no synergistic effect when co-expressing LXRβ and ChREBPα (Supplementary Figure S1A,B). Taken together, these results demonstrate that LXRα but not LXRβ, co-activates the expression of ChREBP-specific target genes in vitro and in vivo together with ChREBPα.

3.3. LXR α :ChREBP α Co-Activation Requires Functional ChoREs But Not LXREs

LXR and ChREBP share many transcriptional targets, for example, the DNL genes *Acc*, *Fasn*, and *Scd1*, which contain both LXREs and ChoREs in their promoter/regulatory regions [3,21]. The ChREBP target genes *Lpk* and *Chrebp β* promoters, however, only contain ChoREs and no canonical LXREs. Analysis of the *Lpk* and *Chrebp β* reporters using *NHR scan* (http://www.cisreg.ca/cgi-bin/NHR-scan/nhr_scan.cgi) suggested one weak candidate in the *Chrebp β* exon 1B promoter. This was, however, discarded after a deletion scan showing no effect on the promoter activity (Supplementary Figure S1C,D; DR4 del). We also remapped the functional ChoRE in the *Chrebp β* exon 1B promoter to the so-called “E-box-like” domain, 98 bases upstream of the TSS (Supplementary Figure S1C,E)—a detail missed in the original ChREBP β paper [37]. Nonetheless, despite no obvious LXRE, LXR α was able to activate the reporters together with ChREBP α (Figure 2A). We therefore investigated the impact of ChoREs and LXREs on LXR α :ChREBP α co-activation by designing three synthetic luciferase reporters: one containing two canonical ChoREs and two canonical LXREs, one that contained only the two ChoREs and one that only contained the two LXREs. The order (ChoRE-LXRE-ChoRE-LXRE) and the phasing (20 bp) of the recognition elements was kept constant (Figure 3A) to make sure that the TFs would adopt the same rotational orientation in all three constructs, as this has been shown to greatly impact transactivity on compound promoters [68]. To ensure an acceptable read-out from the synthetic promoters, we turned to the constitutively active forms of ChREBP, ChREBP β and ChREBP-Q. While ChREBP β is a naturally occurring isoform lacking the LID, ChREBP-Q is a ChREBP α quadruple mutant H51A/S56D/F90A/N278A that has escaped the low-glucose inhibition while keeping the N-terminal domain [32]. As expected, a synergistic co-activation was observed with both LXR α /ChREBP-Q and LXR α /ChREBP β on the ChoRE+LXRE reporter (Figure 3B), reflecting the situation on a dual LXR/ChREBP target gene. Interestingly, this pattern was retained on the ChoRE-only reporter but only with LXR α and ChREBP-Q. ChREBP β seemed to have lost the ability to co-activate with LXR α in this context, mimicking a ChREBP-specific target gene (Figure 3B). This was not due to different abilities to bind to the promoter, as evaluated by ChIP (Supplementary Figure S2A). The effect was even more dramatic on the LXRE-only reporter where neither ChREBP-Q nor ChREBP β was able to activate, even though LXR still transactivated the promoter (Supplementary Figure S2B). This indicates that ChoREs but not LXREs, are sufficient to support LXR α :ChREBP α co-activation and that only full-length ChREBP, that is, not ChREBP β , is co-activated by LXR α on ChoRE-only target genes. To assess this on natural promoters we used the ChREBP-specific, ChoRE-only *Chrebp β* and *Lpk*-driven reporters. Again, the same pattern emerged: LXR α was able to co-activate ChREBP-Q but not ChREBP β that lacks most of the LID (Figure 3C).

3.4. LXR α and ChREBP α Interact via Key Activation Domains

The ability of LXR α to co-activate ChREBP α in an LXRE-independent manner naturally brought up the question of what domains of LXR α and ChREBP α that are involved in their interaction. We therefore examined the interaction between full-length LXR and ChREBP and different truncations using CoIP. ChREBP α interacted with LXR α when immunoprecipitating both ways (Figures 1A and 4A). On the other hand and in line with the gene expression data (Figure 3), ChREBP β did not bind to LXR α as neither ChREBP β nor LXR α was able to co-immunoprecipitate with each other (Figure 4A). ChREBP β lacks the first 177 amino acids (aa) in the N-terminal, which form most of the LID in ChREBP α . Hence, we constructed a ChREBP truncation that only expressed the first 177 residues, that is, the LID. This domain bound strongly to LXR α and seemed sufficient to support the interaction between the full-length factors (Figure 4A). Furthermore, we examined the interactions among ChREBP α and different LXR α truncations. ChREBP α interacted with the LXR α C-terminus, including its hinge domain and LBD (Figure 4B). In addition, ChREBP α also interacted with LXR β (Supplementary Figure S3), although this interaction seems to be less relevant in liver (Figure 2B and Supplementary Figure S1A,B). ChREBP α was previously shown to interact with FXR, with one of the interaction surfaces residing in its LBD [65]. Multiple sequence alignment using ClustalX

(<http://www.clustal.org/clustal2>) revealed that LXR α , LXR β and FXR show high similarity in multiple patches throughout the LBD (data not shown), suggesting that LXR α might use a similar interface when binding to ChREBP α .

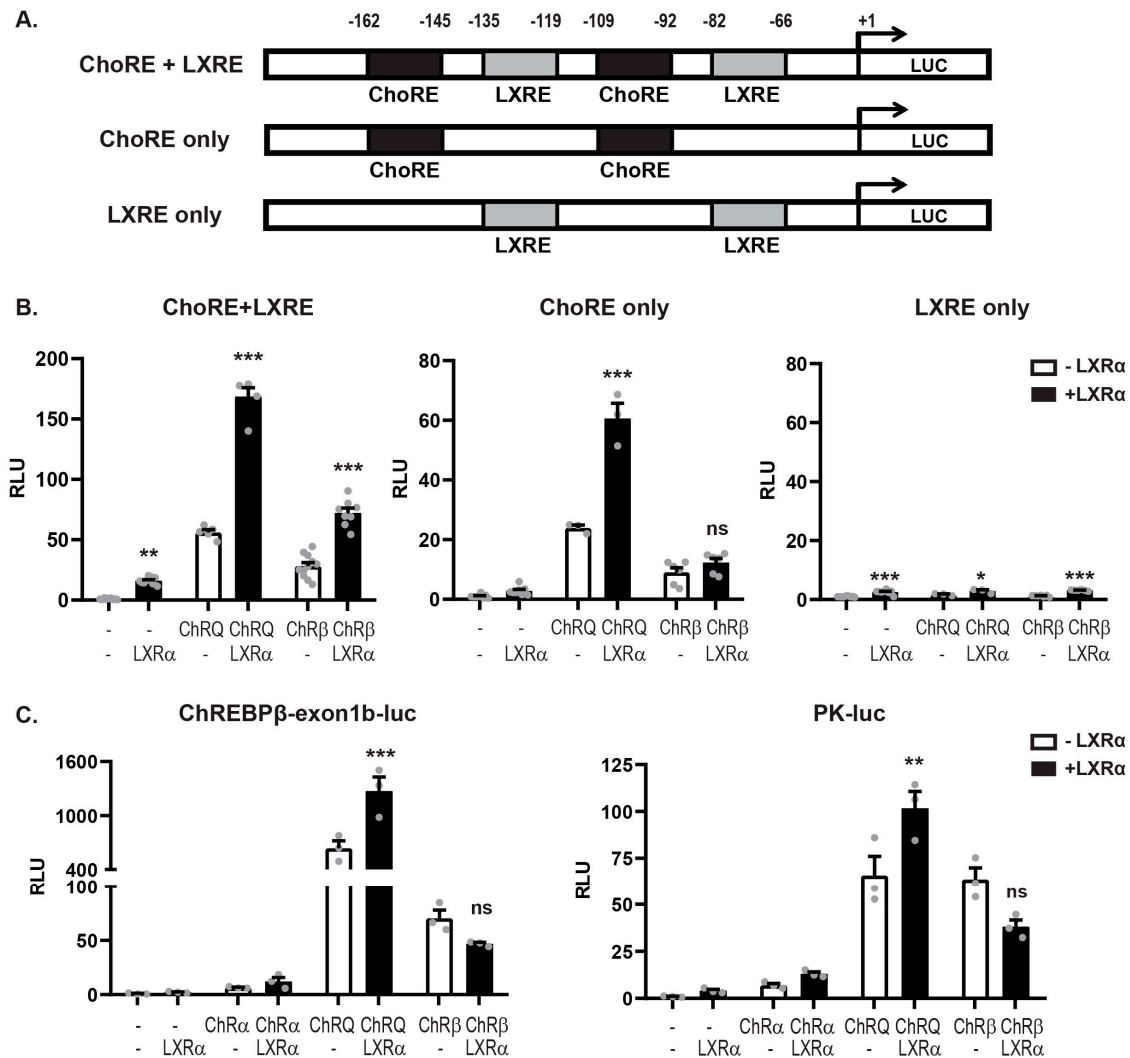


Figure 3. LXR α :ChREBP α co-activation requires functional ChoREs but not LXREs. (A) Schematic representation of the synthetic luciferase reporters constructs. ChoRE, carbohydrate response element; LXRE, LXR response element. (B) Huh7 cells cultured in 25 mM glucose were transfected with synthetic luciferase reporters containing ChoRE+LXRE, ChoRE-only or LXRE-only and plasmids expressing ChREBP α , the activated quadruple mutant ChREBP-Q or ChREBP β , together with Mlx γ , with or without LXR α /RXR α . The Renilla luciferase reporter pRL-CMV was used as internal control. Dual luciferase reporter assays were performed 24 h post transfection. (C) Huh7 cells cultured in 25 mM glucose were transfected with a *Chrebp β* or *Lpk*-driven luciferase reporter and plasmids expressing ChREBP α , ChREBP-Q, ChREBP β together with Mlx γ , with or without LXR α /RXR α . The Renilla luciferase reporter pRL-CMV was used as internal control. Dual luciferase reporter assays were performed 24 h post transfection. Data are presented as mean \pm SEM ($n = 3-7$). Significant differences are shown as * $p < 0.05$, ** $p < 0.01$, *** $p < 0.001$ compared to control within the same ChREBP isoform transfection. ns, not significant.

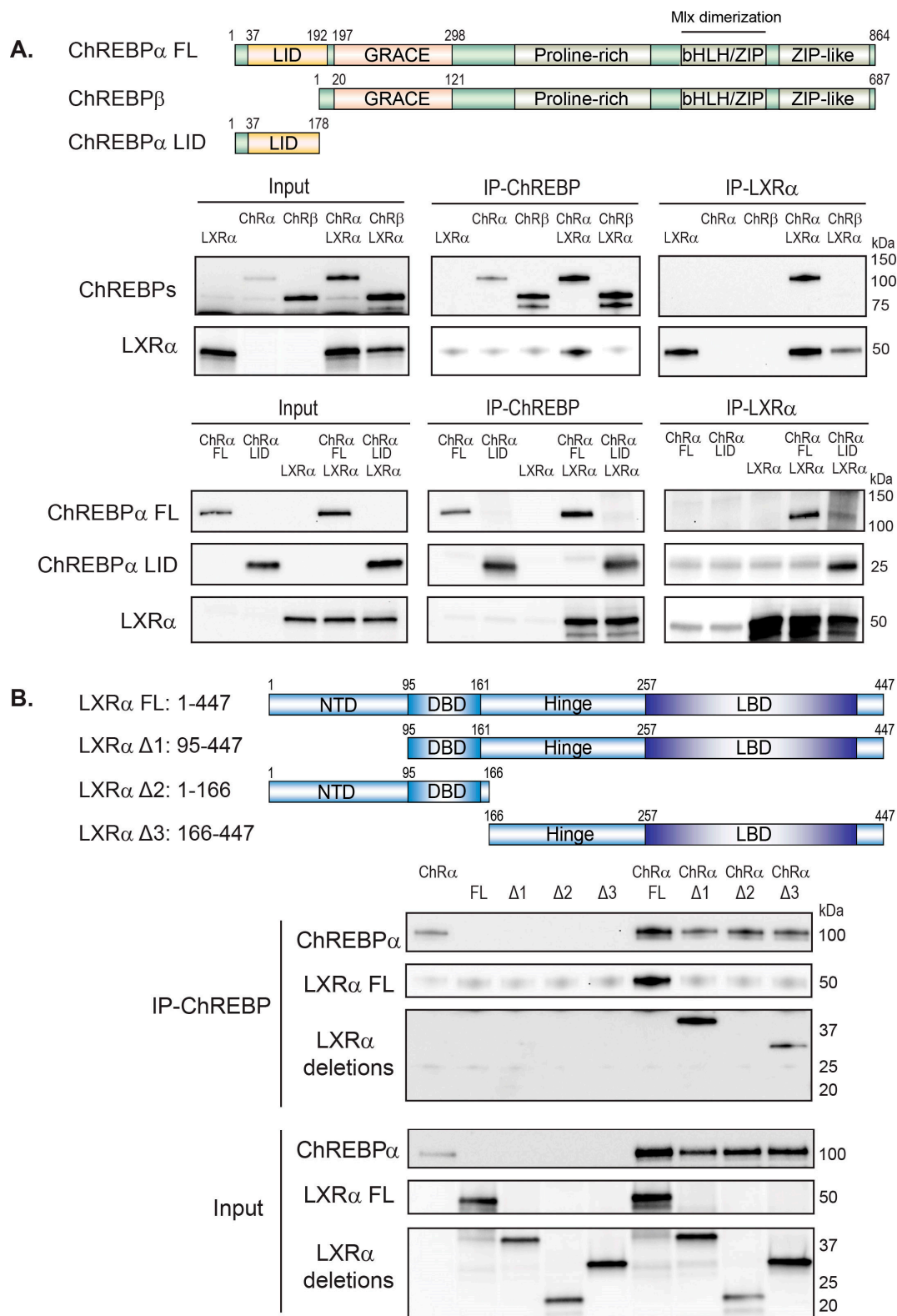


Figure 4. LXR α and ChREBP α interact via key activation domains. (A) Top panel: Schematic representation of the ChREBP α full-length (FL), ChREBP β and the low glucose inhibitory domain (LID) protein. Bottom panel: CoIP of LXR α and ChREBP α , ChREBP β or LID, expressed in COS-1 cells cultured in 25 mM glucose. The ChREBP expression plasmids were transfected with a DNA ratio of ChREBP α :ChREBP β :LID = 1:6:1, to obtain comparable protein levels. Lysates were immunoprecipitated with ChREBP, FLAG (for LID) or LXR α antibodies and input and immunoprecipitated proteins

immunoblotted with the same antibodies ($n = 3$). One representative western blot is shown. LID, low-glucose inhibitory domain; GRACE, glucose-response activation conserved element; bHLH, basic helix-loop-helix domain; ZIP, leucine zipper. (B). Top panel: Schematic representation of the LXR α FL and truncations. Bottom panel: CoIP of ChREBP α and LXR α FL or truncations expressed in COS-1 cells cultured in 25 mM glucose. Lysates were immunoprecipitated with ChREBP antibody ($n = 3$). Input and immunoprecipitated proteins were immunoblotted with ChREBP or FLAG (for LXR α FL and truncations) antibodies. One representative western blot is shown. NTD, N-terminal domain; DBD, DNA-binding domain; LBD, ligand-binding domain.

To expand on the consequences of the ChREBP:LXR interaction in a functional context, we asked whether LXR α is dependent on binding to DNA to induce the activity of ChREBP α on ChREBP target genes, given that the interaction seems to run via LID and LBD. To this end, we constructed an LXR α DNA binding mutant (DBDm), in which two cysteines (C115 and C118) in the first DNA-binding domain (DBD) zinc finger were mutated to alanine to abrogate DNA binding. The LXR α DBD mutant had lost its ability to transactivate the *Srebp1c* promoter as well as the *Lpk* promoter (Supplementary Figure S4A,B), the former being a well-established LXR target gene [55]. Peculiarly, the LXR α DBDm also lacked the ability to co-activate ChREBP α , arguing that DNA binding or rather DBD integrity is important for the full co-activation effect of LXR (Supplementary Figure S4B). This is in line with what we observed in Figure 3B, where the promoter LXRE was mutated and the reporter output amplitude dropped while the regulation pattern was retained. Moreover, it contrasts with the loss of co-regulation seen when the ChoRE was mutated (Supplementary Figure S4B, right panel; Figure 3B, right panel). Taken together, our data suggest that ChREBP α and LXR α interact via key regulatory domains, namely the N-terminal LID of ChREBP α and the C-terminal, LBD-containing part of LXR α . This assigns a novel function to the ChREBP LID in physically bridging the two factors, allowing LXR α to co-activate ChREBP α on ChREBP-specific target genes. Importantly however, our data do not formally exclude the possibility of other factors, like RXR or Mlx, being involved in tethering the two domains.

3.5. Ligand-Activated LXR α Represses ChREBP α Activity on ChREBP-Specific Target Genes

The physical interaction and co-regulatory interplay between ChREBP α and LXR α led us to ask how this affects gene expression in a fully chromatinized context. To investigate this, we isolated primary mouse hepatocytes and cultivated them for 24 h in either low glucose (1 mM) or high glucose (25 mM) to induce ChREBP activity and concomitantly stimulated them with the potent, selective LXR agonist GW3965 (10 μ M) to induce LXR-activity. The DNL genes *Acacb*, *Fasn* and *Scd1*—which are common targets of LXR and ChREBP—were significantly upregulated by the LXR agonist (Figure 5A). The expression of ChREBP-specific target genes *Chrebp β* , *Lpk*, *Txnip* and *Rgs16* on the other hand showed a dramatically different pattern (Figure 5B): These genes were upregulated by high glucose treatment, while the LXR agonist surprisingly displayed a repressive effect under high glucose conditions. This was also seen with the *Chrebp β* reporter (Supplementary Figure S5A). To exclude a possible GW3965 peculiarity, we recapitulated this experiment with the same outcome using Tularik (T0901317), another LXR agonist, both in primary hepatocytes and by transfecting the ChREBP-specific *Lpk* reporter in Huh7 cells (Supplementary Figure S5A,B). These data reveal that ligand-activated LXR α plays distinct roles on different groups of genes, activating common targets of LXR and ChREBP, while repressing ChREBP-specific target genes.

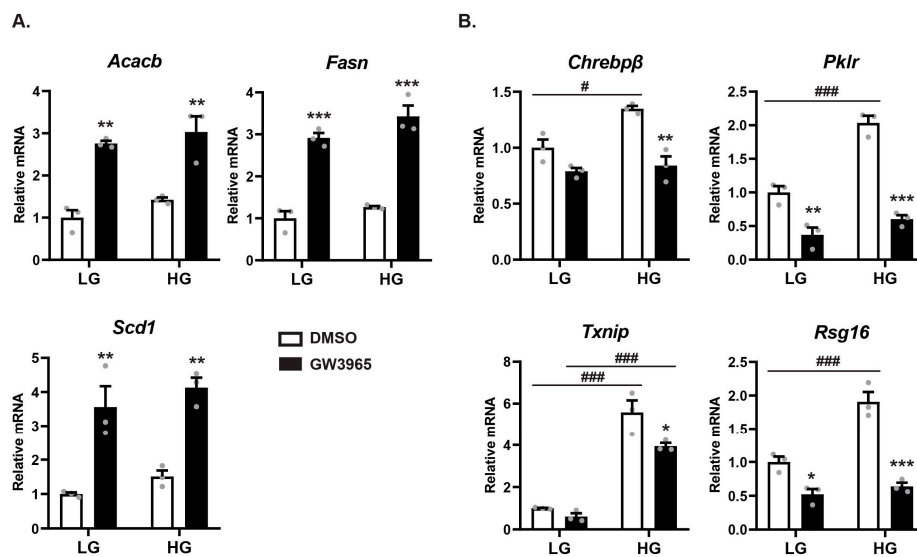


Figure 5. Ligand-activated LXR represses ChREBP α activity on ChREBP-specific target genes. Mouse primary hepatocytes were isolated and cultured in either 1 mM glucose (LG) or 25 mM glucose (HG) for 24 h. For the last 18 h the cells were treated with either DMSO (0.1%) or GW3965 (10 μ M). Expression of (A) DNL genes *Acacb*, *Fasn*, *Scd1* and (B) ChREBP-specific target genes *Chrebp β* (*Mlxipl β*), *Lpk* (*Pklr*), *Txnip* and *Rgs16* was analyzed by quantitative RT-PCR, normalized to *Tbp* and the control group set to 1. The Ct value for *Chrebp β* was \approx 26 for the LG DMSO treatment. Data are presented as mean \pm SEM ($n = 3$). Significant differences are shown as * $p < 0.05$, ** $p < 0.01$, *** $p < 0.001$ compared to DMSO within the same glucose treatment and # $p < 0.01$, ### $p < 0.001$ between LG and HG groups.

3.6. Ligand-Activated LXR α Reduces ChREBP Binding to Chromatin

To try to untangle the mechanism underlying the LXR ligand-dependent repressive effect, we performed ChIP assays to study ChREBP α and LXR α chromatin binding dynamics in the non-cancerous, mouse hepatocyte cell line AML12. Based on our analysis of the ChIP-seq datasets (Figure 1), we selected four gene loci that are co-occupied by ChREBP and LXR in the promoter region: the ChREBP-specific targets *Lpk* and *Txnip* and the common LXR and ChREBP targets *Fasn* and *Scd1* (Figure 6A). The *Mlxipl* exon1b promoter was excluded from these analyses due to low expression of ChREBP β in AML12 cells (data not shown). In the presence of ChREBP α , all four promoters were robustly immunoprecipitated. Moreover, LXR α did not affect ChREBP α occupancy on any of the promoters (Supplementary Figure S6A). Conversely, ChREBP α increased the binding of LXR α on the same promoters (Supplementary Figure S6B), in line with the notion that ChREBP α is able to recruit LXR α to ChoREs via the LID-LBD interaction (Figures 3 and 4).

When the same cells, transfected with both ChREBP α and LXR α , were treated with LXR agonist GW3965, ChREBP α -binding to chromatin was reduced on all four promoters (Figure 6A). Concomitantly, a weak, non-significant reduction was observed for LXR α occupancy. Supporting these observations, GW3965 treatment reduced the ChREBP α :LXR α interaction (Figure 6B), suggesting that a ligand-induced conformational change in LXR α LBD reduces its affinity for ChREBP α . Loss of LXR from the complex weakens ChREBP α 's ability to bind chromatin. This likely has the most dramatic effect on ChREBP-specific target genes, like *Lpk* and *Txnip*, where the LXR binding to the promoter chromatin is mediated through ChREBP (Figure 6A left panel). Common LXR and ChREBP target gene promoters, like *Fasn* and *Scd1*, should still be able to accommodate both factors (Figure 6A). Altogether, this results in the reduced expression of ChREBP-specific target genes seen in Figure 4B. This echoes the lost ChoRE binding and lost feeding-induced expression of ChREBP-specific target genes we previously reported with the LXR double knockout mice [16]. The current data broaden this picture, showing that LXR ligand engagement modulates ChREBP α :LXR α interaction, chromatin occupancy and target gene co-activation.

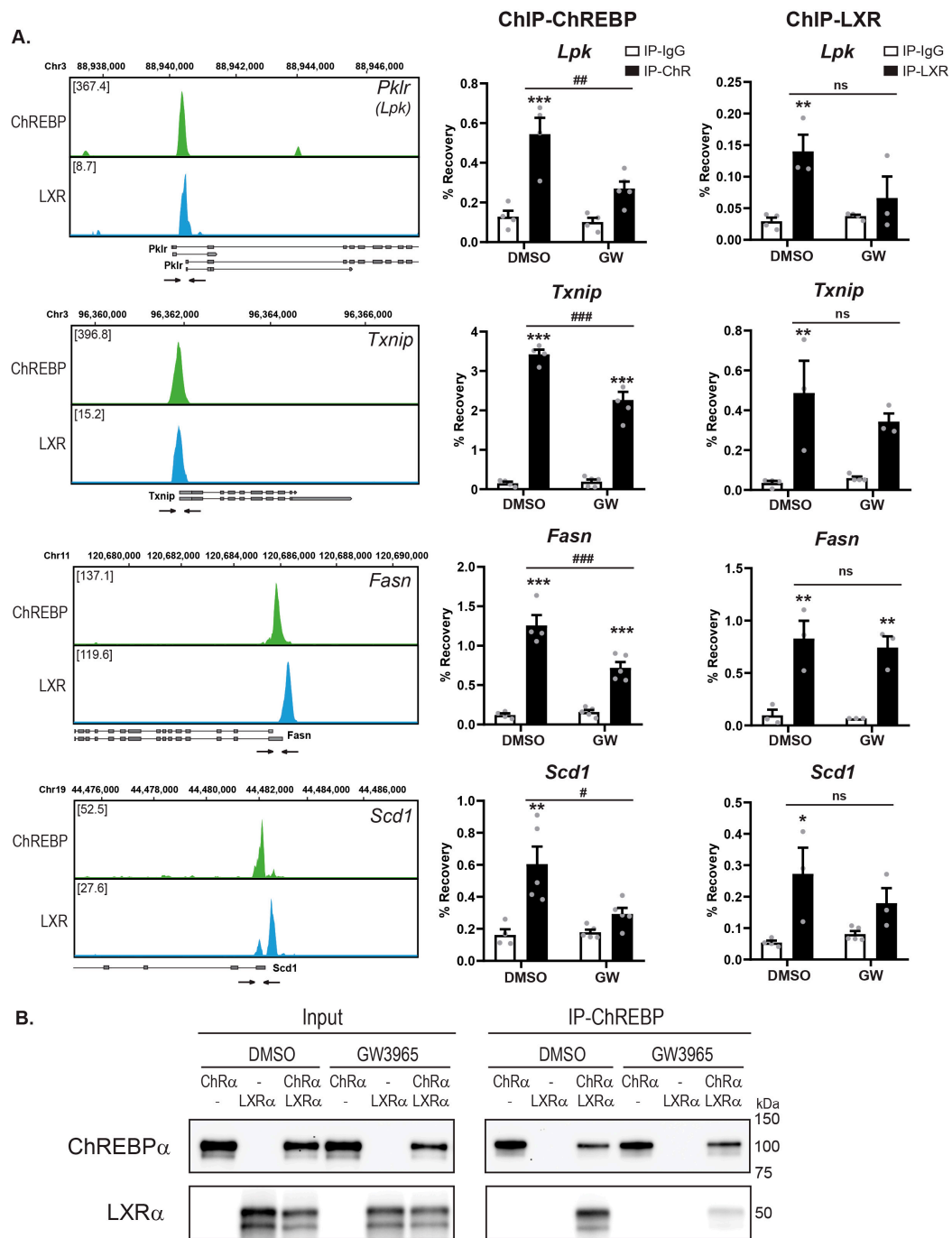


Figure 6. Ligand-activated LXR reduces ChREBP binding to chromatin. (A) Left panels: Local pattern of LXR-ChREBP co-occupancy. Browser view of LXR and ChREBP tracks in the promoter region of *Lpk* (*Pklr*), *Txnip*, *Fasn* and *Scd1*. Square brackets indicate the scale maxima of ChIP/input ratios. Arrows indicate the genomic locations of quantitative RT-PCR primers. Right panel: AML12 cells transfected with ChREBP α /Mlx γ and LXR α /RXR α were treated with DMSO (0.1%) or GW3965 (10 μ M) for 18 h. ChREBP or LXR binding to genomic location indicated in the right panels were detected by ChIP using antibodies against ChREBP, LXR or IgG as negative control. Data are presented as mean \pm SEM ($n = 3-5$). Significant differences are shown as * $p < 0.05$, ** $p < 0.01$, *** $p < 0.001$ compared to ChIP-IgG and # $p < 0.05$, ## $p < 0.01$, ### $p < 0.001$, #### $p < 0.001$ between DMSO and GW3965 groups. ns, not significant. (B) CoIP of LXR α and ChREBP α , expressed in COS-1 cells cultured in 25 mM glucose, treated with DMSO (0.1%) or GW3965 (1 μ M) for 18 h. Lysates were immunoprecipitated with ChREBP antibody ($n = 3$). Input and immunoprecipitated proteins were immunoblotted with ChREBP or LXR α antibodies. One representative western blot is shown.

4. Discussion

Altogether, our findings argue for a close collaboration between LXR α and ChREBP α in regulating glycolytic and lipogenic genes. Hence we propose a new model (Figure 7): Upon glucose signals, the physical interaction between LXR α and ChREBP α allows unliganded LXR α to be recruited to ChoRE-containing promoters and increase ChREBP-specific target gene expression; upon agonist/oxysterol signals, liganded LXR α functions as a molecular switch, disassembling the LXR α :ChREBP α complex and ensuring an adequate restriction of glycolytic and lipogenic target genes.

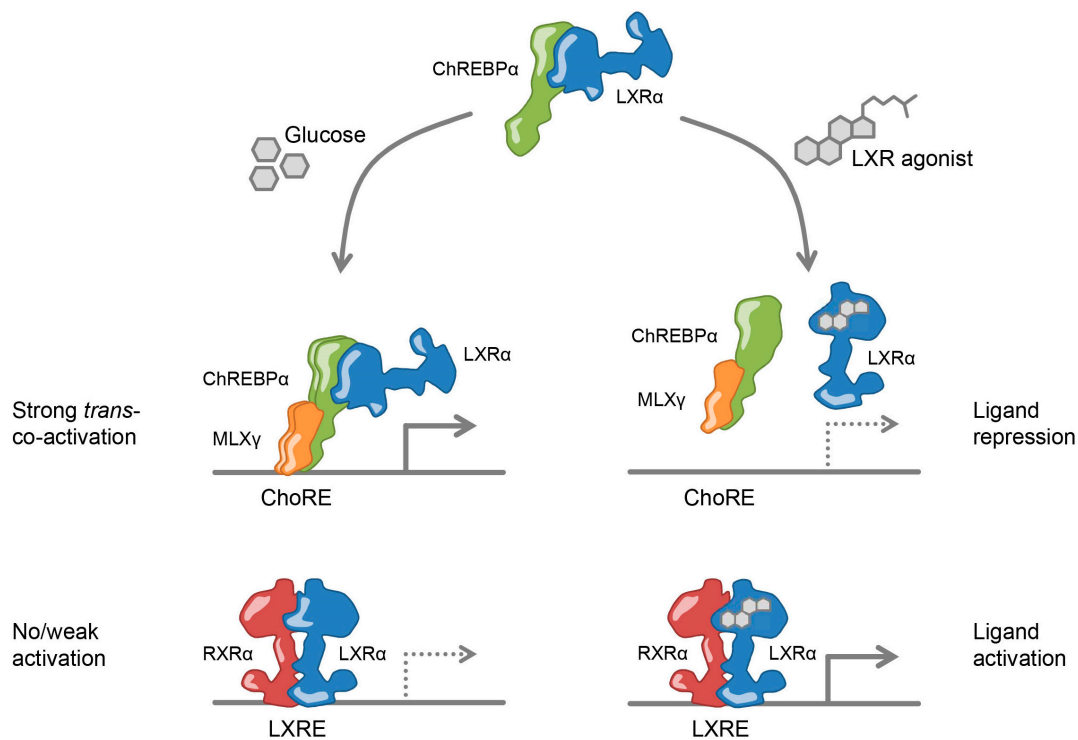


Figure 7. Model of transcriptional co-regulation by LXR α and ChREBP α .

The transcriptional regulation of ChREBP expression by LXR was determined by Cha and Repa already in 2007 [19]. Since then the idea has been that LXR, in addition to regulating its own direct target genes, indirectly contributes to the induction of ChREBP regulated glycolytic and lipogenic target genes. However, in this study we show that the picture is more complex. In addition to upregulating *ChREBP* expression by binding to LXREs and activating the *Mlxipl* promoter, LXR α can directly regulate the transcription of ChREBP α target genes by binding to ChREBP α . With this we propose a new mechanism of action for LXR: *trans-coactivation* (Figure 7). Trans-coactivation resembles transrepression observed with several nuclear receptors (NRs) including GR, PPAR γ , FXR and LXRs [65,69–71], as both mechanisms rely on the NR being tethered to other TFs *in trans*. However, while LXR transrepression of NF κ B and AP-1 is agonist-dependent [71,72], LXR trans-coactivation of ChREBP relies on unliganded LXR (Figure 7). Our findings indicate that LXR might have DNA-binding domain (DBD)-independent function that contributes to its regulation of liver metabolism. This was recently also demonstrated for Rev-erb α , which is tethered to chromatin by hepatic lineage determining TFs [73]. DBD-independent functions like these might explain non-overlapping cistromes and/or transcriptomes in different cell types [43,74]. A relocation of LXR from trans-coactivation complexes on ChREBP-specific target genes to classical ligand-engaged RXR heterodimers on LXR-specific target genes is also in line with the type of TF-cofactor redistribution described for NF κ B [75] and PPAR γ [76]. An LXR-driven redistribution of co-factors between ChREBP-specific and LXR-specific promoters, would also explain the ligand-dependent repression observed in our study. In fact, SREBP-1c could be one of the potential candidates, as LXR, ChREBP and SREBP-1c are tightly interconnected and

coordinately regulate lipogenesis. SREBP-1c is known to compete with PGC1 α for direct interaction with the LBD of HNF-4 [77,78]. Ligand-activated LXR may lead to increased levels of SREBP-1c proteins that potentially could compete with the interaction between LXR and ChREBP.

Posttranslational modification by small ubiquitin-like modifier (SUMO) of TFs and coregulators is generally linked to transcriptional repression [79] and SUMOylation of LXRs and PPAR γ appears to be required for transrepression in macrophages [71]. Phosphorylation and acetylation, which reflect intracellular nutrient availability, modulate ChREBP and LXR transactivity, co-factor recruitment, DNA binding and stability [80,81]. Whether these posttranslational modifications are involved in enforcing the LXR α :ChREBP α complex is not known. If so, O-GlcNAc modification, which derives from the metabolically integrated hexosamine biosynthetic pathway (HBP), might be a candidate. LXR is post-translationally O-GlcNAc modified in response to high glucose [16,18]. The same is true for ChREBP, which leads to increased transcriptional activity and recruitment to target gene promoters [38,39]. Importantly, LXR and the O-GlcNAc transferase (OGT) bind directly to each other and co-localize in the nucleus. Moreover, LXR regulates the O-GlcNAc-modification of ChREBP α [16]. Could LXR α be involved in tethering OGT to ChREBP α and through this mediate O-GlcNAc modification, as reported by Guinez et al. [39] and subsequently cause the synergistic trans-coactivation of ChREBP α target genes shown herein? This is an interesting possibility that would link the nutrient sensor O-GlcNAc and the flux through the HBP even tighter to the cross-regulation of LXR and ChREBP [4,16,40,82].

An important observation in our study is the different ability of ChREBP α and ChREBP β to respond to the LXR α trans-coactivation. While ChREBP α and ChREBP-Q are activated by LXR α and repressed by LXR agonists, ChREBP β is non-responsive to both cues (Figures 2 and 3 and Figure S5). This is due to ChREBP β lacking a functional LID, which directs the interaction with LXR. The LID, located in the ChREBP α N-terminal—also called the MondoA conserved region (MCR)—was originally described as a purely repressive domain [31,83]. However, by mutating the ChREBP α N-terminal Davies et al. showed that this domain is indeed an activation domain kept silent at low glucose conditions [32]. Moreover, they speculated that the MCR1–4 domains (ChREBP aa 1–197) must be interacting with a coregulatory protein that plays a role in transcriptional activation in a step subsequent to glucose-dependent relief of repression [32]. In a bioinformatics sequence-structure analysis approach ChREBP was in fact suggested to interact with NRs, like HNF4 α and FXR but through a nuclear receptor box (NRB) in the proline-rich region (Figure 4A), to support interaction between CBP/p300 and ChREBP MCR6 [33]. Based on our data, we now propose LXR α to be the co-regulator hypothesized by Davies et al. [32]. Moreover, we confirm that ChREBP β has escaped low-glucose control and we expand this to include negative regulation by liganded LXR. As a consequence ChREBP β acts as an extremely potent effector of carbohydrate signals through its feed-forward relationship with ChREBP α and so it is no surprise that its expression levels and stability is much lower than ChREBP α . This has been described before [37,84] and is confirmed in our study (Figure 4).

The high genome-wide co-occupancy of LXR and ChREBP observed in the ChIP-seq data was rather surprising: More than 71% of ChREBP-LXR peak pairs have peaks less than 100 bp apart (Figure 1B), suggesting full co-localization at these sites. A similar frequency of overlapping LXR peaks had been reported before by Boergesen et al. for LXR and PPAR, on non-canonical LXR/PPAR recognition elements (DR4 or DR1) [43]. The existence of LXR-PPAR α heterodimers has been suggested earlier [67] but the authors found no evidence for such transcriptional complexes. Instead they concluded that the receptors bound to the same degenerate elements, representing NR binding hot spots [85], in a mutually exclusive manner [43]. In our study, on the other hand, many of the overlapping LXR and ChREBP peaks are found on or adjacent to ChoREs (in e.g., *Lpk*, *Chrebp β* , *Tixn1p*, *Rgs16*), with no obvious LXRE/DR4 close by. In addition, our data demonstrate a physical interaction between the factors and the ability of ChREBP α to recruit LXR α to the promoter ChoRE but not the other way around. This points to a different mechanism underlying the ChREBP-LXR co-occupancy, where ChREBP α recruits LXR α in trans to ChoREs. Our data do not formally rule out the possibility that LXR α on certain sites also contacts chromatin directly, via its DBD, in addition to binding to

ChREBP α via its LBD. In fact, such ChREBP-LXR contacts might function as bridging point for smaller or larger chromatin loops [86,87], like promoter-enhancer loops [88], possibly within topologically associated domains (TADs) [89]. A tantalizing scenario could be that ChREBP α and LXR α are involved in bridging the exon 1A (*Chrebp α*) and exon 1B (*Chrebp β*) promoter at the *Mlxipl* locus, where ChREBP α binding to the *Chrebp β* promoter could contact LXR α sitting on the *Chrebp α* promoter 17 kb downstream and coordinate the expression from both promoters given different nutritional cues. High glucose would enforce the contact, driving *Chrebp β* expression [37], while high levels of oxidized cholesterol would break the contact and drive *Chrebp α* expression. This type of looping is known for other TFs for example, GATA-1 and its co-factor FOG-1. Both factors are required and need to physically interact to produce a DNA loop bringing the β -globin locus control region (LCR) together with the promoter [90]. Unbiased chromatin capturing techniques [86,91] is warranted to identify LXR-ChREBP trans-coactivation-dependent 3D chromatin contacts.

LXR α and ChREBP α promote glycolytic and lipogenic gene expression in high glucose conditions [3]. High cholesterol in the form of oxysterols, on the other hand, will activate LXR and drive cholesterol metabolism and efflux [92]. In the liver acetyl-CoA generated from β -oxidation of saturated fatty acids (SFAs) is used in cholesterol biosynthesis. Thus, diets rich in SFAs and trans-FAs might cause excess levels of cholesterol that need to be excreted via the bile [93]. While exogenous cholesterol contributes to the total, high cholesterol levels are often a result of or secondary to, high levels of dietary SFAs. This puts some of our observations in an interesting perspective. In the case of a carbohydrate and lipid-rich condition, the liver receives both glucose and oxysterol cues, activating both glucose-driven lipogenesis and oxysterol-driven cholesterol excretion. LXR α , which activates both pathways, also functions as a molecular switch (Figure 7). To prevent toxic accumulation of free cholesterol, *de novo* synthesized FAs is used to esterify cholesterol that are released as neutral cholesteryl esters in apoB-containing lipoproteins [94,95]. However, our data suggest that ligand-bound LXR will reduce the co-activation of glycolytic and lipogenic ChREBP target genes. Accordingly, LXR α might safeguard the liver against ectopic SFA levels. Alternatively, LXR α 's activation-to-repression relay is part of a negative feedback mechanism, ensuring that the activation of ChREBP α , co-activation of *Chrebp β* transcription and subsequent induction of glycolytic and lipogenic genes is limited, when the local concentration of pyruvate, acetyl-CoA and SFAs, as well as cholesterol/oxysterol reaches a certain level. This hitherto unappreciated role of LXR α may have been overlooked due to LXR's DNL-promoting function.

Several LXR-activating drugs have been developed through the years aiming at boosting reverse cholesterol transport [92,96]. However, the use of such agonists has been hampered by their lipogenic effects, leading to hypertriglyceridemia and hepatic steatosis [8,25]. As LXR seem to have both lipogenic-promoting and lipogenic-limiting effects, it is tempting to speculate if it is possible to separate the two. The success of such an effort would most probably lie in targeting both the DBD and LBD of LXR α , breaking the DNA:DBD contact [97,98] and activating the LBD. Preliminary *in vitro* data using the LXR DBD-mutant in combination with GW3965 suggest that this might be a possible approach.

Supplementary Materials: The following are available online at <http://www.mdpi.com/2073-4409/9/5/1214/s1>. Table S1: Cloning primers sequences; Table S2: SYBR primers sequences; Table S3: ChIP primers sequences; Figure S1A: Neither LXR α nor RXR α is able to induce the *Chrebp β* promoter alone; Figure S1B: LXR α but not LXR β , co-activates the expression of ChREBP-specific target genes; Figure S1C–E: The functional ChoRE in the *Chrebp β* exon 1B promoter maps to an E-box-like element; Figure S2A: ChREBP α , - β and -Q all bind to the ChoRE+LXRE reporter; Figure S2B: LXR α transactivates the LXRE only reporter; Figure S3: ChREBP α interacts with LXR β ; Figure S4: DBD integrity is important for full LXR co-activational activity; Figure S5: The LXR agonist Tularik represses ChREBP α activity on ChREBP-specific target genes; Figure S6: Ligand-activated LXR α reduces ChREBP binding to chromatin.

Author Contributions: Conceptualization: Q.F., R.C.N. and T.S.; Data curation: I.G., R.B.L.; Formal analysis: Q.F., I.G., R.B.L. and T.S.; Methodology: Q.F., H.S., J.M., C.B., S.M.U. and T.S.; Investigation: Q.F., R.C.N., C.M.N., C.L., K.V., H.S., J.M., C.B.; Project administration: T.S.; Resources: H.I.N. Funding acquisition: H.I.N., L.M.G.-W., T.S.; Validation: Q.F., T.S.; Visualization: Q.F., I.G. and T.S.; Supervision: O.S.G., L.M.G.-W., T.S.; Writing—original draft: Q.F. and T.S.; Writing—review & editing: all co-authors. All authors have read and agreed to the published version of the manuscript.

Funding: This research was funded by grants from the University of Oslo, the Throne Holst Foundation, the Novo Nordic Foundation and the Anders Jahres Foundation.

Acknowledgments: The authors thank Lawrence Chan (Baylor College of Medicine, Houston) for providing the ChIP-ChREBP dataset and thank Susanne Mandrup (University of Southern Denmark) for providing the ChIP-LXR dataset. The authors thank Mark Herman (Duke University), Em. Howard Towle (University of Minnesota), Donald K. Scott (Icahn School of Medicine at Mount Sinai) and Nobuhiro Yamada (University of Tsukuba) for kindly providing plasmids.

Conflicts of Interest: The authors declare that they have no known competing financial interests or personal relationships that could have appeared to influence the work reported in this paper.

Abbreviations

ACC, acetyl-CoA carboxylase; ChoRE, carbohydrate response element; ChREBP, carbohydrate responsive element-binding protein; ChIP-seq, chromatin immunoprecipitation-sequencing; CoIP, co-immunoprecipitation; DBD, ligand-binding domain; DNL, *de novo* lipogenesis; DOKO, double knockout; FXR, farnesoid X receptor; GRACE, glucose response activation conserved element; GSEA, gene set enrichment analysis; HBP, hexosamine biosynthetic pathway; LCR, locus control region; LID, low glucose inhibitory domain; LBD, ligand-binding domain; LPK, liver pyruvate kinase; LXR, liver X receptor; LXREs, LXR response elements; MLX, Max-like protein X; NRs, nuclear receptors; NRB, nuclear receptor box; O-GlcNAc, O-linked β -N-acetylglucosamine; OGT, O-GlcNAc transferase; PPAR, peroxisome proliferator-activated receptor; RXR, retinoid X receptor; SCD1, stearoyl-CoA desaturase-1; SFAs, saturated fatty acids; SREBP-1c, sterol regulatory element-binding protein-1c; SUMO, small ubiquitin-like modifier; TADs, topologically associated domains; TFs, transcription factors; TSS, transcription start site.

References

1. Ballestri, S.; Zona, S.; Targher, G.; Romagnoli, D.; Baldelli, E.; Nascimbeni, F.; Roverato, A.; Guaraldi, G.; Lonardo, A. Nonalcoholic fatty liver disease is associated with an almost twofold increased risk of incident type 2 diabetes and metabolic syndrome. Evidence from a systematic review and meta-analysis. *J. Gastroenterol. Hepatol.* **2016**, *31*, 936–944. [[CrossRef](#)] [[PubMed](#)]
2. Samuel, V.T.; Shulman, G.I. Nonalcoholic Fatty Liver Disease as a Nexus of Metabolic and Hepatic Diseases. *Cell Metab.* **2018**, *27*, 22–41. [[CrossRef](#)] [[PubMed](#)]
3. Grønning-Wang, L.M.; Bindesbøll, C.; Nebb, H.I. The Role of Liver X Receptor in Hepatic *de novo* Lipogenesis and Cross-Talk with Insulin and Glucose Signaling. In *Lipid Metabolism*; Baez, R.V., Ed.; INTECH Open Access: London, UK, 2013; pp. 61–90.
4. Poupeau, A.; Postic, C. Cross-regulation of hepatic glucose metabolism via ChREBP and nuclear receptors. *Biochim. Biophys. Acta* **2011**, *1812*, 995–1006. [[CrossRef](#)] [[PubMed](#)]
5. Jakobsson, T.; Treuter, E.; Gustafsson, J.A.; Steffensen, K.R. Liver X receptor biology and pharmacology: New pathways, challenges and opportunities. *Trends Pharmacol. Sci.* **2012**, *33*, 394–404. [[CrossRef](#)] [[PubMed](#)]
6. Repa, J.J.; Mangelsdorf, D.J. The role of orphan nuclear receptors in the regulation of cholesterol homeostasis. *Annu. Rev. Cell Dev. Biol.* **2000**, *16*, 459–481. [[CrossRef](#)] [[PubMed](#)]
7. Zhang, Y.; Breevoort, S.R.; Angdisen, J.; Fu, M.; Schmidt, D.R.; Holmstrom, S.R.; Kliewer, S.A.; Mangelsdorf, D.J.; Schulman, I.G. Liver LXRA expression is crucial for whole body cholesterol homeostasis and reverse cholesterol transport in mice. *J. Clin. Investig.* **2012**, *122*, 1688–1699. [[CrossRef](#)] [[PubMed](#)]
8. Schultz, J.R.; Tu, H.; Luk, A.; Repa, J.J.; Medina, J.C.; Li, L.; Schwendner, S.; Wang, S.; Thoolen, M.; Mangelsdorf, D.J.; et al. Role of LXRs in control of lipogenesis. *Genes Dev.* **2000**, *14*, 2831–2838. [[CrossRef](#)] [[PubMed](#)]
9. Laffitte, B.A.; Chao, L.C.; Li, J.; Walczak, R.; Hummasti, S.; Joseph, S.B.; Castrillo, A.; Wilpitz, D.C.; Mangelsdorf, D.J.; Collins, J.L.; et al. Activation of liver X receptor improves glucose tolerance through coordinate regulation of glucose metabolism in liver and adipose tissue. *Proc. Natl. Acad. Sci. USA* **2003**, *100*, 5419–5424. [[CrossRef](#)]
10. Gonzalez, N.; Bensinger, S.J.; Hong, C.; Beceiro, S.; Bradley, M.N.; Zelcer, N.; Deniz, J.; Ramirez, C.; Diaz, M.; Gallardo, G.; et al. Apoptotic cells promote their own clearance and immune tolerance through activation of the nuclear receptor LXR. *Immunity* **2009**, *31*, 245–258. [[CrossRef](#)]
11. Willy, P.J.; Umesonon, K.; Ong, E.S.; Evans, R.M.; Heyman, R.A.; Mangelsdorf, D.J. LXR, a nuclear receptor that defines a distinct retinoid response pathway. *Genes Dev.* **1995**, *9*, 1033–1045. [[CrossRef](#)]

12. Janowski, B.A.; Willy, P.J.; Devi, T.R.; Falck, J.R.; Mangelsdorf, D.J. An oxysterol signalling pathway mediated by the nuclear receptor LXR alpha. *Nature* **1996**, *383*, 728–731. [[CrossRef](#)] [[PubMed](#)]
13. Svensson, S.; Ostberg, T.; Jacobsson, M.; Norstrom, C.; Stefansson, K.; Hallen, D.; Johansson, I.C.; Zachrisson, K.; Ogg, D.; Jendeborg, L. Crystal structure of the heterodimeric complex of LXRalpha and RXRbeta ligand-binding domains in a fully agonistic conformation. *EMBO J.* **2003**, *22*, 4625–4633. [[CrossRef](#)] [[PubMed](#)]
14. Jin, L.; Li, Y. Structural and functional insights into nuclear receptor signaling. *Adv. Drug Deliv. Rev.* **2010**, *62*, 1218–1226. [[CrossRef](#)] [[PubMed](#)]
15. Hu, X.; Li, S.; Wu, J.; Xia, C.; Lala, D.S. Liver X receptors interact with corepressors to regulate gene expression. *Mol. Endocrinol.* **2003**, *17*, 1019–1026. [[CrossRef](#)] [[PubMed](#)]
16. Bindsboll, C.; Fan, Q.; Norgaard, R.C.; MacPherson, L.; Ruan, H.B.; Wu, J.; Pedersen, T.A.; Steffensen, K.R.; Yang, X.; Matthews, J.; et al. Liver X receptor regulates hepatic nuclear O-GlcNAc signaling and carbohydrate responsive element-binding protein activity. *J. Lipid Res.* **2015**, *56*, 771–785. [[CrossRef](#)] [[PubMed](#)]
17. Chen, G.; Liang, G.; Ou, J.; Goldstein, J.L.; Brown, M.S. Central role for liver X receptor in insulin-mediated activation of Srebp-1c transcription and stimulation of fatty acid synthesis in liver. *Proc. Natl. Acad. Sci. USA* **2004**, *101*, 11245–11250. [[CrossRef](#)]
18. Anthonisen, E.H.; Berven, L.; Holm, S.; Nygard, M.; Nebb, H.I.; Gronning-Wang, L.M. Nuclear receptor liver X receptor is O-GlcNAc-modified in response to glucose. *J. Biol. Chem.* **2010**, *285*, 1607–1615. [[CrossRef](#)]
19. Cha, J.Y.; Repa, J.J. The liver X receptor (LXR) and hepatic lipogenesis. The carbohydrate-response element-binding protein is a target gene of LXR. *J. Biol. Chem.* **2007**, *282*, 743–751. [[CrossRef](#)]
20. Repa, J.J.; Liang, G.; Ou, J.; Bashmakov, Y.; Lobaccaro, J.M.; Shimomura, I.; Shan, B.; Brown, M.S.; Goldstein, J.L.; Mangelsdorf, D.J. Regulation of mouse sterol regulatory element-binding protein-1c gene (SREBP-1c) by oxysterol receptors, LXRalpha and LXRbeta. *Genes Dev.* **2000**, *14*, 2819–2830. [[CrossRef](#)]
21. Filhoulaud, G.; Guilmeau, S.; Dentin, R.; Girard, J.; Postic, C. Novel insights into ChREBP regulation and function. *Trends Endocrinol. Metab.* **2013**, *24*, 257–268. [[CrossRef](#)]
22. Talukdar, S.; Hillgartner, F.B. The mechanism mediating the activation of acetyl-coenzyme A carboxylase-alpha gene transcription by the liver X receptor agonist T0-901317. *J. Lipid Res.* **2006**, *47*, 2451–2461. [[CrossRef](#)] [[PubMed](#)]
23. Mitro, N.; Mak, P.A.; Vargas, L.; Godio, C.; Hampton, E.; Molteni, V.; Kreuzsch, A.; Saez, E. The nuclear receptor LXR is a glucose sensor. *Nature* **2007**, *445*, 219–223. [[CrossRef](#)] [[PubMed](#)]
24. Collins, J.L.; Fivush, A.M.; Watson, M.A.; Galardi, C.M.; Lewis, M.C.; Moore, L.B.; Parks, D.J.; Wilson, J.G.; Tippin, T.K.; Binz, J.G.; et al. Identification of a nonsteroidal liver X receptor agonist through parallel array synthesis of tertiary amines. *J. Med. Chem.* **2002**, *45*, 1963–1966. [[CrossRef](#)] [[PubMed](#)]
25. Fievet, C.; Staels, B. Liver X receptor modulators: Effects on lipid metabolism and potential use in the treatment of atherosclerosis. *Biochem. Pharmacol.* **2009**, *77*, 1316–1327. [[CrossRef](#)]
26. Fessler, M.B. The challenges and promise of targeting the Liver X Receptors for treatment of inflammatory disease. *Pharmacol. Ther.* **2018**, *181*, 1–12. [[CrossRef](#)]
27. Yamashita, H.; Takenoshita, M.; Sakurai, M.; Bruick, R.K.; Henzel, W.J.; Shillinglaw, W.; Arnot, D.; Uyeda, K. A glucose-responsive transcription factor that regulates carbohydrate metabolism in the liver. *Proc. Natl. Acad. Sci. USA* **2001**, *98*, 9116–9121. [[CrossRef](#)]
28. Ma, L.; Sham, Y.Y.; Walters, K.J.; Towle, H.C. A critical role for the loop region of the basic helix-loop-helix/leucine zipper protein Mlx in DNA binding and glucose-regulated transcription. *Nucleic Acids Res.* **2007**, *35*, 35–44. [[CrossRef](#)]
29. Ma, L.; Tsatsos, N.G.; Towle, H.C. Direct role of ChREBP.Mlx in regulating hepatic glucose-responsive genes. *J. Biol. Chem.* **2005**, *280*, 12019–12027. [[CrossRef](#)]
30. Shih, H.M.; Liu, Z.; Towle, H.C. Two CACGTG motifs with proper spacing dictate the carbohydrate regulation of hepatic gene transcription. *J. Biol. Chem.* **1995**, *270*, 21991–21997. [[CrossRef](#)]
31. Li, M.V.; Chang, B.; Imamura, M.; Pongvarin, N.; Chan, L. Glucose-dependent transcriptional regulation by an evolutionarily conserved glucose-sensing module. *Diabetes* **2006**, *55*, 1179–1189. [[CrossRef](#)]
32. Davies, M.N.; O’Callaghan, B.L.; Towle, H.C. Activation and repression of glucose-stimulated ChREBP requires the concerted action of multiple domains within the MondoA conserved region. *Am. J. Physiol. Endocrinol. Metab.* **2010**, *299*, E665–E674. [[CrossRef](#)] [[PubMed](#)]

33. McFerrin, L.G.; Atchley, W.R. A novel N-terminal domain may dictate the glucose response of Mondo proteins. *PLoS ONE* **2012**, *7*, e34803. [[CrossRef](#)] [[PubMed](#)]
34. Kawaguchi, T.; Takenoshita, M.; Kabashima, T.; Uyeda, K. Glucose and cAMP regulate the L-type pyruvate kinase gene by phosphorylation/dephosphorylation of the carbohydrate response element binding protein. *Proc. Natl. Acad. Sci. USA* **2001**, *98*, 13710–13715. [[CrossRef](#)]
35. Kabashima, T.; Kawaguchi, T.; Wadzinski, B.E.; Uyeda, K. Xylulose 5-phosphate mediates glucose-induced lipogenesis by xylulose 5-phosphate-activated protein phosphatase in rat liver. *Proc. Natl. Acad. Sci. USA* **2003**, *100*, 5107–5112. [[CrossRef](#)] [[PubMed](#)]
36. Dentin, R.; Tomas-Cobos, L.; Foufelle, F.; Leopold, J.; Girard, J.; Postic, C.; Ferre, P. Glucose 6-phosphate, rather than xylulose 5-phosphate, is required for the activation of ChREBP in response to glucose in the liver. *J. Hepatol.* **2012**, *56*, 199–209. [[CrossRef](#)] [[PubMed](#)]
37. Herman, M.A.; Peroni, O.D.; Villoria, J.; Schon, M.R.; Abumrad, N.A.; Bluher, M.; Klein, S.; Kahn, B.B. A novel ChREBP isoform in adipose tissue regulates systemic glucose metabolism. *Nature* **2012**, *484*, 333–338. [[CrossRef](#)]
38. Sakiyama, H.; Fujiwara, N.; Noguchi, T.; Eguchi, H.; Yoshihara, D.; Uyeda, K.; Suzuki, K. The role of O-linked GlcNAc modification on the glucose response of ChREBP. *Biochem. Biophys. Res. Commun.* **2010**, *402*, 784–789. [[CrossRef](#)]
39. Guinez, C.; Filhoulaud, G.; Rayah-Benamed, F.; Marmier, S.; Dubuquoy, C.; Dentin, R.; Moldes, M.; Burnol, A.F.; Yang, X.; Lefebvre, T.; et al. O-GlcNAcylation increases ChREBP protein content and transcriptional activity in the liver. *Diabetes* **2011**, *60*, 1399–1413. [[CrossRef](#)]
40. Fan, Q.; Norgaard, R.C.; Bindesboll, C.; Lucas, C.; Dalen, K.T.; Babaie, E.; Itkonen, H.M.; Matthews, J.; Nebb, H.I.; Gronning-Wang, L.M. LXRA α Regulates Hepatic ChREBP α Activity and Lipogenesis upon Glucose, but Not Fructose Feeding in Mice. *Nutrients* **2017**, *9*, 678. [[CrossRef](#)]
41. Ducheix, S.; Montagner, A.; Polizzi, A.; Lasserre, F.; Regnier, M.; Marmugi, A.; Benamed, F.; Bertrand-Michel, J.; Mselli-Lakhal, L.; Loiseau, N.; et al. Dietary oleic acid regulates hepatic lipogenesis through a liver X receptor-dependent signaling. *PLoS ONE* **2017**, *12*, e0181393. [[CrossRef](#)]
42. Pongvarin, N.; Chang, B.; Imamura, M.; Chen, J.; Moolsuwan, K.; Sae-Lee, C.; Li, W.; Chan, L. Genome-Wide Analysis of ChREBP Binding Sites on Male Mouse Liver and White Adipose Chromatin. *Endocrinology* **2015**, *156*, 1982–1994. [[CrossRef](#)] [[PubMed](#)]
43. Boergesen, M.; Pedersen, T.A.; Gross, B.; van Heeringen, S.J.; Hagenbeek, D.; Bindesboll, C.; Caron, S.; Lalloyer, F.; Steffensen, K.R.; Nebb, H.I.; et al. Genome-wide profiling of liver X receptor, retinoid X receptor, and peroxisome proliferator-activated receptor α in mouse liver reveals extensive sharing of binding sites. *Mol. Cell. Biol.* **2012**, *32*, 852–867. [[CrossRef](#)] [[PubMed](#)]
44. Amemiya, H.M.; Kundaje, A.; Boyle, A.P. The ENCODE Blacklist: Identification of Problematic Regions of the Genome. *Sci. Rep.* **2019**, *9*, 9354. [[CrossRef](#)] [[PubMed](#)]
45. Furio-Tari, P.; Conesa, A.; Tarazona, S. RGMATCH: Matching genomic regions to proximal genes in omics data integration. *BMC Bioinformatics* **2016**, *17*, 427. [[CrossRef](#)] [[PubMed](#)]
46. Sandve, G.K.; Gundersen, S.; Rydbeck, H.; Glad, I.K.; Holden, L.; Holden, M.; Liestol, K.; Clancy, T.; Ferkingstad, E.; Johansen, M.; et al. The Genomic HyperBrowser: Inferential genomics at the sequence level. *Genome Biol.* **2010**, *11*, R121. [[CrossRef](#)]
47. Alberti, S.; Schuster, G.; Parini, P.; Feltkamp, D.; Diczfalusy, U.; Rudling, M.; Angelin, B.; Bjorkhem, I.; Pettersson, S.; Gustafsson, J.A. Hepatic cholesterol metabolism and resistance to dietary cholesterol in LXRB β -deficient mice. *J. Clin. Investig.* **2001**, *107*, 565–573. [[CrossRef](#)]
48. Schuster, G.U.; Parini, P.; Wang, L.; Alberti, S.; Steffensen, K.R.; Hansson, G.K.; Angelin, B.; Gustafsson, J.A. Accumulation of foam cells in liver X receptor-deficient mice. *Circulation* **2002**, *106*, 1147–1153. [[CrossRef](#)]
49. Faul, F.; Erdfelder, E.; Lang, A.G.; Buchner, A. G*Power 3: A flexible statistical power analysis program for the social, behavioral, and biomedical sciences. *Behav. Res. Methods* **2007**, *39*, 175–191. [[CrossRef](#)]
50. Arnesen, H.; Haj-Yasein, N.N.; Tungen, J.E.; Soedling, H.; Matthews, J.; Paulsen, S.M.; Nebb, H.I.; Sylte, I.; Hansen, T.V.; Saether, T. Molecular modelling, synthesis, and biological evaluations of a 3,5-disubstituted isoxazole fatty acid analogue as a PPAR α -selective agonist. *Bioorg. Med. Chem.* **2019**, *27*, 4059–4068. [[CrossRef](#)]
51. Nakabayashi, H.; Taketa, K.; Miyano, K.; Yamane, T.; Sato, J. Growth of human hepatoma cells lines with differentiated functions in chemically defined medium. *Cancer Res.* **1982**, *42*, 3858–3863.

52. Weedon-Fekjaer, M.S.; Dalen, K.T.; Solaas, K.; Staff, A.C.; Duttaroy, A.K.; Nebb, H.I. Activation of LXR increases acyl-CoA synthetase activity through direct regulation of ACSL3 in human placental trophoblast cells. *J. Lipid Res.* **2010**, *51*, 1886–1896. [[CrossRef](#)]
53. Thompson, K.S.; Towle, H.C. Localization of the carbohydrate response element of the rat L-type pyruvate kinase gene. *J. Biol. Chem.* **1991**, *266*, 8679–8682.
54. Collier, J.J.; Zhang, P.; Pedersen, K.B.; Burke, S.J.; Haycock, J.W.; Scott, D.K. c-Myc and ChREBP regulate glucose-mediated expression of the L-type pyruvate kinase gene in INS-1-derived 832/13 cells. *Am. J. Physiol. Endocrinol. Metab.* **2007**, *293*, E48–E56. [[CrossRef](#)] [[PubMed](#)]
55. Yoshikawa, T.; Shimano, H.; Amemiya-Kudo, M.; Yahagi, N.; Hasty, A.H.; Matsuzaka, T.; Okazaki, H.; Tamura, Y.; Iizuka, Y.; Ohashi, K.; et al. Identification of liver X receptor-retinoid X receptor as an activator of the sterol regulatory element-binding protein 1c gene promoter. *Molecul. Cell. Biol.* **2001**, *21*, 2991–3000. [[CrossRef](#)] [[PubMed](#)]
56. Bindsbøll, C.; Grønning-Wang, L.M. Liver X receptors connect nuclear O-GlcNAc signaling to hepatic glucose utilization and lipogenesis. *Recept. Clin. Investig.* **2015**, *2*, e897.
57. Ye, J.; Coulouris, G.; Zaretskaya, I.; Cutcutache, I.; Rozen, S.; Madden, T.L. Primer-BLAST: A tool to design target-specific primers for polymerase chain reaction. *BMC Bioinform.* **2012**, *13*, 134. [[CrossRef](#)] [[PubMed](#)]
58. Herwig, R.; Hardt, C.; Lienhard, M.; Kamburov, A. Analyzing and interpreting genome data at the network level with ConsensusPathDB. *Nat. Protoc.* **2016**, *11*, 1889–1907. [[CrossRef](#)] [[PubMed](#)]
59. Koudritsky, M.; Domany, E. Positional distribution of human transcription factor binding sites. *Nucleic Acids Res.* **2008**, *36*, 6795–6805. [[CrossRef](#)]
60. Xie, X.; Lu, J.; Kulbokas, E.J.; Golub, T.R.; Mootha, V.; Lindblad-Toh, K.; Lander, E.S.; Kellis, M. Systematic discovery of regulatory motifs in human promoters and 3' UTRs by comparison of several mammals. *Nature* **2005**, *434*, 338–345. [[CrossRef](#)]
61. Chong, H.K.; Infante, A.M.; Seo, Y.K.; Jeon, T.I.; Zhang, Y.; Edwards, P.A.; Xie, X.; Osborne, T.F. Genome-wide interrogation of hepatic FXR reveals an asymmetric IR-1 motif and synergy with LRH-1. *Nucleic Acids Res.* **2010**, *38*, 6007–6017. [[CrossRef](#)]
62. Stender, J.D.; Kim, K.; Charn, T.H.; Komm, B.; Chang, K.C.; Kraus, W.L.; Benner, C.; Glass, C.K.; Katzenellenbogen, B.S. Genome-wide analysis of estrogen receptor alpha DNA binding and tethering mechanisms identifies Runx1 as a novel tethering factor in receptor-mediated transcriptional activation. *Mol. Cell. Biol.* **2010**, *30*, 3943–3955. [[CrossRef](#)] [[PubMed](#)]
63. Ijssennagger, N.; Janssen, A.W.F.; Milona, A.; Ramos Pittol, J.M.; Hollman, D.A.A.; Mokry, M.; Betzel, B.; Berends, F.J.; Janssen, I.M.; van Mil, S.W.C.; et al. Gene expression profiling in human precision cut liver slices in response to the FXR agonist obeticholic acid. *J. Hepatol.* **2016**, *64*, 1158–1166. [[CrossRef](#)] [[PubMed](#)]
64. Salvatore, S.; Dagestad Rand, K.; Grytten, I.; Ferkingstad, E.; Domanska, D.; Holden, L.; Gheorghe, M.; Mathelier, A.; Glad, I.; Kjetil Sandve, G. Beware the Jaccard: The choice of similarity measure is important and non-trivial in genomic colocalisation analysis. *Brief. Bioinform.* **2019**. [[CrossRef](#)] [[PubMed](#)]
65. Caron, S.; Huaman Samanez, C.; Dehondt, H.; Ploton, M.; Briand, O.; Lien, F.; Dorchies, E.; Dumont, J.; Postic, C.; Cariou, B.; et al. Farnesoid X receptor inhibits the transcriptional activity of carbohydrate response element binding protein in human hepatocytes. *Mol. Cell. Biol.* **2013**, *33*, 2202–2211. [[CrossRef](#)]
66. Trabelsi, M.S.; Daoudi, M.; Prawitt, J.; Ducastel, S.; Touche, V.; Sayin, S.I.; Perino, A.; Brighton, C.A.; Sebt, Y.; Kluza, J.; et al. Farnesoid X receptor inhibits glucagon-like peptide-1 production by enteroendocrine L cells. *Nat. Commun.* **2015**, *6*, 7629. [[CrossRef](#)]
67. Ide, T.; Shimano, H.; Yoshikawa, T.; Yahagi, N.; Amemiya-Kudo, M.; Matsuzaka, T.; Nakakuki, M.; Yatoh, S.; Iizuka, Y.; Tomita, S.; et al. Cross-talk between peroxisome proliferator-activated receptor (PPAR) alpha and liver X receptor (LXR) in nutritional regulation of fatty acid metabolism. II. LXRs suppress lipid degradation gene promoters through inhibition of PPAR signaling. *Mol. Endocrinol.* **2003**, *17*, 1255–1267. [[CrossRef](#)]
68. Molvaersmyr, A.K.; Saether, T.; Gilfillan, S.; Lorenzo, P.I.; Kvaloy, H.; Matre, V.; Gabrielsen, O.S. A SUMO-regulated activation function controls synergy of c-Myb through a repressor-activator switch leading to differential p300 recruitment. *Nucleic Acids Res.* **2010**, *38*, 4970–4984. [[CrossRef](#)]
69. De Bosscher, K.; Beck, I.M.; Dejager, L.; Bougarne, N.; Gaigneaux, A.; Chateauvieux, S.; Ratman, D.; Bracke, M.; Tavernier, J.; Vanden Berghe, W.; et al. Selective modulation of the glucocorticoid receptor can distinguish between transrepression of NF-kappaB and AP-1. *Cell. Mol. Life Sci.* **2014**, *71*, 143–163. [[CrossRef](#)]

70. Li, M.; Pascual, G.; Glass, C.K. Peroxisome proliferator-activated receptor gamma-dependent repression of the inducible nitric oxide synthase gene. *Mol. Cell. Biol.* **2000**, *20*, 4699–4707. [[CrossRef](#)]
71. Ghisletti, S.; Huang, W.; Ogawa, S.; Pascual, G.; Lin, M.E.; Willson, T.M.; Rosenfeld, M.G.; Glass, C.K. Parallel SUMOylation-dependent pathways mediate gene- and signal-specific transrepression by LXRs and PPARgamma. *Mol. Cell* **2007**, *25*, 57–70. [[CrossRef](#)]
72. Huang, W.; Ghisletti, S.; Saijo, K.; Gandhi, M.; Aouadi, M.; Tesz, G.J.; Zhang, D.X.; Yao, J.; Czech, M.P.; Goode, B.L.; et al. Coronin 2A mediates actin-dependent de-repression of inflammatory response genes. *Nature* **2011**, *470*, 414–418. [[CrossRef](#)] [[PubMed](#)]
73. Zhang, Y.; Fang, B.; Emmett, M.J.; Damle, M.; Sun, Z.; Feng, D.; Armour, S.M.; Remsberg, J.R.; Jager, J.; Soccio, R.E.; et al. GENE REGULATION. Discrete functions of nuclear receptor Rev-erbalpha couple metabolism to the clock. *Science* **2015**, *348*, 1488–1492. [[CrossRef](#)] [[PubMed](#)]
74. Heinz, S.; Benner, C.; Spann, N.; Bertolino, E.; Lin, Y.C.; Laslo, P.; Cheng, J.X.; Murre, C.; Singh, H.; Glass, C.K. Simple combinations of lineage-determining transcription factors prime cis-regulatory elements required for macrophage and B cell identities. *Mol. Cell* **2010**, *38*, 576–589. [[CrossRef](#)] [[PubMed](#)]
75. Schmidt, S.F.; Larsen, B.D.; Loft, A.; Nielsen, R.; Madsen, J.G.; Mandrup, S. Acute TNF-induced repression of cell identity genes is mediated by NFkappaB-directed redistribution of cofactors from super-enhancers. *Genome Res.* **2015**, *25*, 1281–1294. [[CrossRef](#)]
76. Step, S.E.; Lim, H.W.; Marinis, J.M.; Prokesch, A.; Steger, D.J.; You, S.H.; Won, K.J.; Lazar, M.A. Anti-diabetic rosiglitazone remodels the adipocyte transcriptome by redistributing transcription to PPARgamma-driven enhancers. *Genes Dev.* **2014**, *28*, 1018–1028. [[CrossRef](#)]
77. Yamamoto, T.; Shimano, H.; Nakagawa, Y.; Ide, T.; Yahagi, N.; Matsuzaka, T.; Nakakuki, M.; Takahashi, A.; Suzuki, H.; Sone, H.; et al. SREBP-1 interacts with hepatocyte nuclear factor-4 alpha and interferes with PGC-1 recruitment to suppress hepatic gluconeogenic genes. *J. Biol. Chem.* **2004**, *279*, 12027–12035. [[CrossRef](#)]
78. Ponugoti, B.; Fang, S.; Kemper, J.K. Functional interaction of hepatic nuclear factor-4 and peroxisome proliferator-activated receptor-gamma coactivator 1alpha in CYP7A1 regulation is inhibited by a key lipogenic activator, sterol regulatory element-binding protein-1c. *Mol. Endocrinol.* **2007**, *21*, 2698–2712. [[CrossRef](#)]
79. Flotho, A.; Melchior, F. Sumoylation: A regulatory protein modification in health and disease. *Annu. Rev. Biochem.* **2013**, *82*, 357–385. [[CrossRef](#)]
80. Abdul-Wahed, A.; Guilmeau, S.; Postic, C. Sweet Sixteenth for ChREBP: Established Roles and Future Goals. *Cell Metab.* **2017**, *26*, 324–341. [[CrossRef](#)]
81. Becares, N.; Gage, M.C.; Pineda-Torra, I. Posttranslational Modifications of Lipid-Activated Nuclear Receptors: Focus on Metabolism. *Endocrinology* **2017**, *158*, 213–225. [[CrossRef](#)]
82. Hardiville, S.; Hart, G.W. Nutrient regulation of signaling, transcription, and cell physiology by O-GlcNAcylation. *Cell Metab.* **2014**, *20*, 208–213. [[CrossRef](#)] [[PubMed](#)]
83. Pongvarin, N.; Lee, J.K.; Yechoor, V.K.; Li, M.V.; Assavapokee, T.; Suksaranjit, P.; Thepsongwajja, J.J.; Saha, P.K.; Oka, K.; Chan, L. Carbohydrate response element-binding protein (ChREBP) plays a pivotal role in beta cell glucotoxicity. *Diabetologia* **2012**, *55*, 1783–1796. [[CrossRef](#)] [[PubMed](#)]
84. Jing, G.; Chen, J.; Xu, G.; Shalev, A. Islet ChREBP-beta is increased in diabetes and controls ChREBP-alpha and glucose-induced gene expression via a negative feedback loop. *Mol. Metab.* **2016**, *5*, 1208–1215. [[CrossRef](#)] [[PubMed](#)]
85. Siersbaek, R.; Nielsen, R.; John, S.; Sung, M.H.; Baek, S.; Loft, A.; Hager, G.L.; Mandrup, S. Extensive chromatin remodelling and establishment of transcription factor ‘hotspots’ during early adipogenesis. *EMBO J.* **2011**, *30*, 1459–1472. [[CrossRef](#)]
86. Mora, A.; Sandve, G.K.; Gabrielsen, O.S.; Eskeland, R. In the loop: Promoter-enhancer interactions and bioinformatics. *Brief. Bioinform.* **2016**, *17*, 980–995. [[CrossRef](#)]
87. West, A.G.; Gaszner, M.; Felsenfeld, G. Insulators: Many functions, many mechanisms. *Genes Dev.* **2002**, *16*, 271–288. [[CrossRef](#)]
88. Siersbaek, R.; Madsen, J.G.S.; Javierre, B.M.; Nielsen, R.; Bagge, E.K.; Cairns, J.; Wingett, S.W.; Traynor, S.; Spivakov, M.; Fraser, P.; et al. Dynamic Rewiring of Promoter-Anchored Chromatin Loops during Adipocyte Differentiation. *Mol. Cell* **2017**, *66*, 420–435. [[CrossRef](#)]

89. Paulsen, J.; Liyakat Ali, T.M.; Nekrasov, M.; Delbarre, E.; Baudement, M.O.; Kurscheid, S.; Tremethick, D.; Collas, P. Long-range interactions between topologically associating domains shape the four-dimensional genome during differentiation. *Nat. Genet.* **2019**, *51*, 835–843. [[CrossRef](#)]
90. Vakoc, C.R.; Letting, D.L.; Gheldof, N.; Sawado, T.; Bender, M.A.; Groudine, M.; Weiss, M.J.; Dekker, J.; Blobel, G.A. Proximity among distant regulatory elements at the beta-globin locus requires GATA-1 and FOG-1. *Mol. Cell* **2005**, *17*, 453–462. [[CrossRef](#)]
91. Dekker, J.; Marti-Renom, M.A.; Mirny, L.A. Exploring the three-dimensional organization of genomes: Interpreting chromatin interaction data. *Nat. Rev. Genet.* **2013**, *14*, 390–403. [[CrossRef](#)]
92. Naik, S.U.; Wang, X.; Da Silva, J.S.; Jaye, M.; Macphee, C.H.; Reilly, M.P.; Billheimer, J.T.; Rothblat, G.H.; Rader, D.J. Pharmacological activation of liver X receptors promotes reverse cholesterol transport in vivo. *Circulation* **2006**, *113*, 90–97. [[CrossRef](#)] [[PubMed](#)]
93. Zhu, R.; Ou, Z.; Ruan, X.; Gong, J. Role of liver X receptors in cholesterol efflux and inflammatory signaling (review). *Mol. Med. Rep.* **2012**, *5*, 895–900. [[CrossRef](#)] [[PubMed](#)]
94. Furbee, J.W., Jr.; Francone, O.; Parks, J.S. In vivo contribution of LCAT to apolipoprotein B lipoprotein cholesteryl esters in LDL receptor and apolipoprotein E knockout mice. *J. Lipid Res.* **2002**, *43*, 428–437. [[PubMed](#)]
95. Xie, C.; Woollett, L.A.; Turley, S.D.; Dietschy, J.M. Fatty acids differentially regulate hepatic cholesteryl ester formation and incorporation into lipoproteins in the liver of the mouse. *J. Lipid Res.* **2002**, *43*, 1508–1519. [[CrossRef](#)]
96. Repa, J.J.; Turley, S.D.; Lobaccaro, J.A.; Medina, J.; Li, L.; Lustig, K.; Shan, B.; Heyman, R.A.; Dietschy, J.M.; Mangelsdorf, D.J. Regulation of absorption and ABC1-mediated efflux of cholesterol by RXR heterodimers. *Science* **2000**, *289*, 1524–1529. [[CrossRef](#)]
97. Moore, T.W.; Mayne, C.G.; Katzenellenbogen, J.A. Minireview: Not picking pockets: Nuclear receptor alternate-site modulators (NRAMs). *Mol. Endocrinol.* **2010**, *24*, 683–695. [[CrossRef](#)]
98. Leung, C.H.; Chan, D.S.; Ma, V.P.; Ma, D.L. DNA-binding small molecules as inhibitors of transcription factors. *Med. Res. Rev.* **2013**, *33*, 823–846. [[CrossRef](#)]



© 2020 by the authors. Licensee MDPI, Basel, Switzerland. This article is an open access article distributed under the terms and conditions of the Creative Commons Attribution (CC BY) license (<http://creativecommons.org/licenses/by/4.0/>).